To the Graduate Council:

I am submitting herewith a thesis written by Cheri Whitehead Clavier entitled "Sol-Gel Monoliths for Optical Copper (II) Determination." I have examined the final paper copy of this thesis for form and content and recommend that it be accepted in partial fulfillment of the requirements for the degree of Master of Science, with a major in Chemistry.

Ziling (Ben) Xue, Major Professor

We have read this thesis
and recommend its acceptance:

Craig E. Barnes

S. Douglass Gilman

Accepted for the Council:

Vice Provost and Dean of Graduate Students

SOL-GEL MONOLITHS FOR OPTICAL COPPER (II) DETERMINATION

A Thesis

Presented for the

Master of Science

Degree

The University of Tennessee, Knoxville

Cheri Whitehead Clavier

December 2001

DEDICATION

This thesis is dedicated to my parents,

who have given me invaluable educational opportunities,

and to my husband and the rest of my family

from whom I draw support, love, and encouragement.

ACKNOWLEDGEMENTS

Throughout the years I have spent at the University of Tennessee, I have met several people to whom I owe my gratitude and appreciation for making my time here so rewarding. I first acknowledge my research advisor, Dr. Ziling (Ben) Xue, for his supervision and guidance, and for his persistence in achieving and maintaining high standards and an admirable work ethic. I would also like to thank the members of my committee, Dr. Craig E. Barnes and Dr. S. Douglass Gilman, for their guidance and careful reading of this thesis, as well as Dr. Xiaobing Feng of the UT Mathematics Department for his assistance with many of the equations mentioned in the appendix. This research was made possible by the financial support of the University of Tennessee and the Measurement and Control Engineering Center at UTK and its member companies.

I have been fortunate to work with a wonderful group of people during my time here, including my sol-gel co-workers: Leonardo Allain, Andrew Canada, Bryan Fagan, Hee-Jung Im, Lynn Rodman, Dr. Joseph Sinski, Alicia Vogt, Dr. Yvette Yang, and Terry Yost, as well as several other lab mates, both past and present. I have enjoyed working with all of you and will miss our daily interactions. I am especially grateful for the many friendships I have made here, specifically Tianniu Chen, Brandi Murray, Angela Whisnant, and Jeffrey Williams. Finally, I include a very special

thanks to Jaime Blanton and Lynn Rodman. I will miss our lunchtime bets and Friday night ritual, but I know I will consider you both good friends for the rest of my life.

Last but certainly not least, my greatest debt is owed to my family, without whose support I could never have achieved this accomplishment. To my parents, Jeff and Gail Lyons and Keith and Susan Whitehead, I love you and will always appreciate that you instilled in me the importance of a quality education. To John, I love you more than I could ever express, and I am so thankful that you understood exactly how difficult this task really was and always supported me every step of the way. Thanks to Benji for always making me laugh, and thanks to the family I married into for your support as well. Papaw Ray, Nana, Papaw John, and Granny Grace---thanks for loving me and always encouraging me. Finally, this list would not be complete without acknowledging the three little "people" who can always make me smile, no matter how badly things in my world are going: Garcia, Raven, and Dixie. Their never-ending antics have helped me understand how simple and wonderful life can be.

ABSTRACT

Heavy metal ions are used in a variety of industrial applications and many are considered pollutants. Currently, metal ion concentration measurements are determined off-site, using techniques that are costly, time-consuming, and inconvenient. This work describes the development of optical Cu^{2+} sensors prepared through the sol-gel process. Initial work was carried out exploring the basic properties of sol-gel glasses with amine ligands incorporated directly into the sol-gel matrix. The sol-gel process was modified to produce physically robust, optically transparent, crack-free sol-gel monoliths incorporating either diamine $NH_2(CH_2)_2NH(CH_2)_3Si(OMe_3)_3$ or monoamine $H_2N(CH_2)_3Si(OMe)_3$ directly into the sol-gel matrix using $Si(OMe)_4$ as a cross-linking agent. The kinetics of cupric ion uptake by the gels in Cu^{2+} solutions of various concentrations was studied by measuring the change in the absorbance of the blue metal:ligand complexes within the gels over time using UV-VIS spectrophotometry. A simple correlation between the rate of complex formation and $[Cu^{2+}]$ in solution was observed. The gels containing diamine ligand could not be regenerated, and could therefore only be used as one-time Cu^{2+} probes, possibly in environmental applications. The gels containing monoamine ligand could be regenerated with EDTA and used in subsequent Cu^{2+} uptake-removal cycles, and thus showed potential as industrial Cu^{2+} ion sensors.

TABLE OF CONTENTS

Chapter			Page
1	INTRODUCTION AND BACKGROUND		1
	1.1	Copper in Industry and the Environment	1
		1.1.1 Electroplating of Copper	2
		1.1.2 Copper and the Microelectronics Industry	4
		1.1.3 Copper in Biological Systems and the Environment	7
	1.2	Chemical Sensing	9
	1.3	The Sol-Gel Process	12
	1.4	Ultraviolet/Visible Absorption Spectrometry	18
	1.5	Brunauer-Emmett-Teller Gas Adsorption Analysis	29
	1.6	Scanning Electron Microscopy	33
	1.7	Overview of this Thesis	36
2	PHYSICIALLY ROBUST, OPTICALLY TRANSPARENT SOL-GEL MONOLITHS GRAFTED WITH DIAMINE LIGANDS FOR SINGLE-USE COPPER (II) DETERMINATION		37
	2.1	Introduction	37
	2.2	Experimental Section	41

Chapter Page

2.2.1 Unsuccessful Attempts to Prepare a Stable Sol-Gel Monolith. 42

2.2.1.a Spin-Coating Sols onto Glass Slides (*Gel Series 2-A*). 43

2.2.1.b Preparation of Monoliths in Cuvettes (*Gel Series 2-B*). 44

2.2.1.c Preparation of Monoliths in Glass Vials (*Gel Series 2-C*). 45

2.2.1.d Preparation of Monoliths in Petri Dishes (*Gel Series 2-D*). 45

2.2.2 The Ligand-Grafting Technique. 47

2.2.2.a Preparation of a Blank Sol-Gel Monolith (*Gel 2-E*). 47

2.2.2.b Preparation of a Ligand-Grafted Sol-Gel Monolith (*Gel 2-F*). 48

2.2.3 Characterization Studies. 49

2.2.4 Spectroscopic Measurements. 51

2.2.5 Cu^{2+} Removal. 52

2.2.6 Reproducibility Study. 52

2.3 Results and Discussion. 52

Chapter Page

2.3.1 Preparation of a Ligand-Grafted Sol-Gel Monolith (*Gel 2-F*). 53

2.3.2 Characterization by BET and SEM. 55

2.3.3 Cu^{2+} Uptake and Determination. 59

2.3.4 Cu^{2+} Removal and Sensor Regeneration. 67

2.3.5 Decreasing Analysis Time. 68

2.4 Conclusions. 68

3 IMPRINTED, MONOAMINE LIGAND-GRAFTED SOL-GEL MONOLITHS FOR MULTICYCLE COPPER (II) DETERMINATION. 72

3.1 Introduction. 72

3.2 Experimental Section. 76

3.2.1 Preparation of a Blank Sol-Gel Monolith (*Gel 3-A*). 76

3.2.2 Preparation of a Ligand-Grafted Sol-Gel Monolith (*Gel 3-B*). 77

3.2.3 Preparation of an Imprinted, Ligand-Grafted Monolith (*Gel 3-C*). 78

3.2.4 Characterization Studies. 79

3.2.5 Spectroscopic Measurements. 79

3.2.6 Cu^{2+} Removal. 81

Chapter Page

3.2.7 Reproducibility Study. 81

3.3 Results and Discussion. 82

3.3.1 Preparation of a Crack-Free, Imprinted, Ligand-Grafted Sol-Gel Monolith (*Gel 3-C*). 82

3.3.2 Characterization by BET and SEM. 86

3.3.3 Cu^{2+} Uptake and Sensing. 90

3.3.4 Cu^{2+} Removal and Sensor Regeneration. 99

3.4 Conclusions. 100

4 CONCLUSIONS AND FUTURE STUDIES. 103

4.1 Conclusions. 103

4.2 Future Studies. 104

REFERENCES. 107

APPENDIX. 115

References for the Appendix. 125

VITA. 126

LIST OF FIGURES

Figure		Page
1.1	Schematic of conventional electroplating.	3
1.2	The steps involved in semiconductor fabrication.	6
1.3	The sol-gel reactions.	14
1.4	The acid-catalyzed mechanism in the sol-gel process.	15
1.5	The base-catalyzed mechanism in the sol-gel process.	16
1.6	Bifunctionalized amine ligands chosen as the sensing element on a solid state sol-gel support.	19
1.7	A typical single-beam spectrophotometer.	21
1.8	Diagram of a Czerny-Turner grating monochromator.	22
1.9	Schematic representation of a charge coupled device (CCD). .	24
1.10	Top: Schematic of an optical fiber. Bottom: Path of light in a waveguide.	25
1.11	Instrumental design used in the current studies.	27
1.12	Schematic of a scanning electron microscope.	34
2.1	Schematic of the preparation of the diamine ligand-grafted *gel 2-F*.	50
2.2	10 point BET plot for diamine ligand-grafted *gel 2-F*.	56

Figure Page

2.3 BET pore size distribution for diamine ligand-grafted *gel 2-F*. 57

2.4 N_2 gas adsorption/desorption isotherms for diamine ligand-grafted *gel 2-F*. 58

2.5 SEM images of diamine ligand-grafted *gel 2-F* at (a) 150,000X and (b) 180,000X magnification. 60

2.6 Absorbance spectra of a typical diamine ligand-grafted *gel 2-F* in 75.03 mM Cu^{2+} from 2-12 min. 61

2.7 Absorbance spectra of $Cu[TMSen]_n^{2+}$ complexes. 63

2.8 Absorbance vs. time plots of diamine ligand-grafted *gels 2-F* in various $[Cu^{2+}]$ from 2-12 min. 64

2.9 Correlation between slopes *dA/dt* from 2-12 min and $[Cu^{2+}]$ for diamine ligand-grafted *gels 2-F*. 65

2.10 Absorbance vs. time plots of diamine ligand-grafted *gels 2-F* in various $[Cu^{2+}]$ from 2-4 min. 69

2.11 Correlation between slopes *dA/dt* from 2-4 min and $[Cu^{2+}]$ for diamine ligand-grafted *gels 2-F*. 70

3.1 Schematic of the preparation of the imprinted, monoamine ligand-grafted *gel 3-C*. 80

3.2 Conventional grafting (non-imprinting) procedure. 84

3.3 Imprint coating procedure. 85

Figure Page

3.4 10 point BET plot for imprinted, monoamine ligand-grafted *gel 3-C*. 87

3.5 BET pore size distribution for imprinted, monoamine ligand-grafted *gel 3-C*. 88

3.6 N_2 gas adsorption/desorption isotherms for imprinted, monoamine ligand-grafted *gel 3-C*. 89

3.7 SEM images of imprinted, monoamine ligand-grafted *gel 3-C* at (a) 45,000X and (b) 130,000X magnification. 91

3.8 Absorbance spectra of a typical imprinted, monoamine ligand-grafted *gel 3-C* in 75.03 mM Cu^{2+} from 2-12 min. 92

3.9 Absorbance spectra of $Cu[H_2N(CH_2)_3Si(OMe)_3]_4^{2+}$, $Cu[EDTA]^{2+}$, and $CuCl_2$ complexes. 93

3.10 Absorbance vs. time plots of imprinted, monoamine ligand-grafted *gels 3-C* in various $[Cu^{2+}]$ from 2-12 min. 95

3.11 Correlation between slopes *dA/dt* from 2-12 min and $[Cu^{2+}]$ for imprinted, monoamine ligand-grafted *gels 3-C*. 97

3.12 Difference in the correlation between *dA/dt* and $[Cu^{2+}]$ when the absorbance maximum is measured at several different wavelengths. 98

A.1 Dimensions of a sol-gel sensor disk. 117

NOMENCLATURE

α	acceptable angle
A	absorbance
Å	angstroms
β	stability constant
b	pathlength
C	BET constant
°C	degrees Celsius
c	concentration
cc	cubic centimeters
cm	centimeter
ε	molar absorbtivity
g	grams
h	hour
i	intercept
K	Kelvin
λ	wavelength
L	liters
L-	ligand
M	molar

M	molecular weight
M^{n+}	metal ion
mg	milligram
µL	microliter
µM	micromolar
mm	millimeter
mM	millimolar
mmol	millimole
min	minute
N	Avogadro's number
n	refractive index
nm	nanometers
P	power
R	ideal gas constant
R^2	regression coefficient
r	radius
S	surface area
s	second
s	slope
T	temperature
t	time

θ	critical angle
V	volts
V	volume
W	weight
X	times

LIST OF ABBREVIATIONS

A/D	analog-to-digital
BET	Brunauer-Emmett-Teller
CCD	charge-coupled device
CRT	cathode-ray tube
CTAB	cetyltrimethylammonium bromide
diamine	N-[3-(trimethoxysilyl)propyl]ethylenediamine
en	ethylenediamine
EPA	Environmental Protection Agency
IR	infrared
MeOH	methanol
monoamine	3-aminopropyltrimethoxysilane
PVC	poly(vinyl chloride)
RCRA	Resource Conservation and Recovery Act
rpm	rotations per minute
SEM	Scanning Electron Microscopy
TMOS	tetramethyl orthosilicate
TMSen	N-[3-(trimethoxysilyl)propyl]ethylenediamine
UV	ultraviolet

CHAPTER ONE

INTRODUCTION AND BACKGROUND

1.1 Copper in Industry and the Environment

Humans first began using copper over 10,000 years ago. Early civilizations found that it could easily be hammered into sheets and worked into complex shapes. By 3000 BC, tin was added to copper to produce the harder bronze,[1] making a wide range of castings possible and ushering in the Bronze Age. The ability to resist corrosion ensured that copper and its alloys were used for both functional and decorative purposes during the Middle Ages through the Industrial Revolution and on to the present day.[2] Large-scale copper mining in the US began in the late 1800's primarily in the West, and the American copper industry is still active today through mining, smelting, refining, and fabricating.[3] The unique properties of copper, including its durability, ductility, malleability, and electrical and thermal conductivity, make possible a wide variety of applications. Today, the world uses approximately 15×10^6 tons of copper each year. The largest use of copper (65%) is in electronic applications such as electrical wire and cable, while another 15% is used in building and construction, including plumbing, roofing, and fittings. The remaining 20% is used in miscellaneous

applications such as air-conditioning and refrigeration, machine parts, and the production of alloys.[4]

1.1.1 Electroplating of Copper

Electroplating is the process of coating a surface with a metal by electric current.[5] Industrially, it is used to prevent rust and corrosion, to provide electrical conductivity or insulation, as a base for soldering operations, and for decorative purposes. A schematic of an electroplating system is shown in **Figure 1.1**. The electrolyte consists of an aqueous salt of the metal to be applied, as well as chemical additives to adjust the conductivity of the bath or control pH. Two electrodes (4-12 V) are immersed in the plating bath. The cathode is the material that is to be plated, and the anode is usually a slab of the plating metal, which maintains the concentration of the metal ion in the bath. When power is applied, the positively charged metal ions deposit out of the bath and onto the cathode. The dissociation of water releases H_2 (g) at the cathode and O_2 (g) at the anode.[6]

Copper is one of the most widely used metals in the electroplating industry. Three types of baths are commonly used for electrodepositing copper:[5]

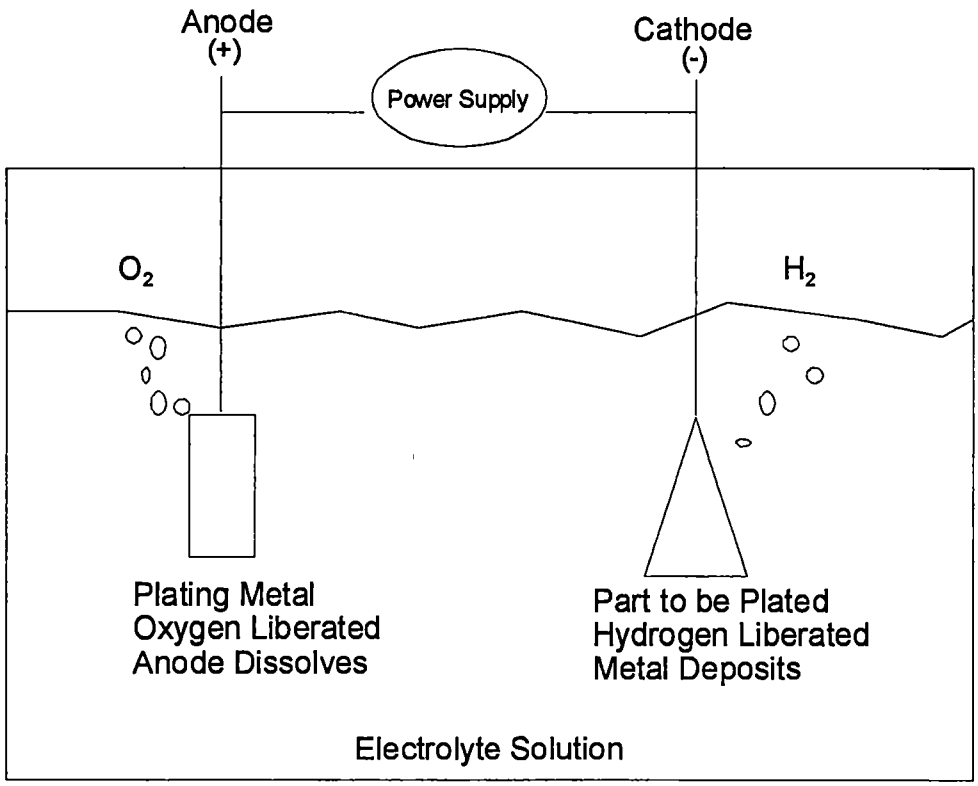

Figure 1.1. Schematic of conventional electroplating.

Adapted from: Burgess, W. A. *Recognition of Health Hazards in Industry*; John Wiley and Sons: New York, 1995.

(a) *Acid copper bath:* Acid copper baths are possibly the most common in copper electroplating, and are often used in electronic printing circuits. These baths are economical, simple in composition, and easy to operate. The simplest acid copper bath contains 150-250 g/L of $CuSO_4$ and 45-75 g/L of sulfuric acid.[5]

(b) *Cyanide copper bath:* A cyanide bath is most often used when the object to be plated is made of steel, since other types of baths will not allow the copper to adhere. It is also used when complex shapes must be plated, since the cyanide bath has such a large throwing power. Generally, this bath contains 22 g/L of copper cyanide, 35 g/L of sodium cyanide, and 15g/L of sodium carbonate.[7] Because cyanide is extremely toxic and the bath emits hydrocyanic gas, great caution must be observed during both plating and waste disposal.

(c) *Pyrophosphate copper bath:* This type of bath is mainly a safer alternative to the cyanide bath. It typically contains 62-106 g/L of copper pyrophosphate ($Cu_2P_2O_7 \cdot 3H_2O$), as well as potassium pyrophosphate and ammonia. This system is prone to organic impurities, and is not often used.[5]

1.1.2 Copper and the Microelectronics Industry

Microelectronics refers to the miniaturization of electronic circuits and components within the semiconductor industry. Electrical circuits are

fabricated by building insulating, conducting, and semiconducting layers on a substrate, typically silicon. A six-inch silicon wafer can hold up to 150 separate integrated circuits, and the major steps in the manufacture of these circuits are shown in **Figure 1.2**. The silicon surface is cleaned and oxidized to form the first insulating layer. A photoresist polymer film, which loses its resistance to chemical etching when exposed to light, is then placed on the surface, and the surface is irradiated with UV light through a photomask that defines the portions of the wafer for treatment. The UV radiation cross-links the polymer, which forms an image of the projected pattern. The portions of the photoresist blocked from the UV light are softened with a developer and washed off the surface. The silicon dioxide layer exposed through this process is removed to expose the silicon surface. By adding dopants, the exposed silicon can be modified to define electrical characteristics or junctions. The remaining photoresist is then removed, and the layer is covered with an insulating silicon oxide coating. This series of steps is repeated again and again, and the layers are connected by depositing a conductive metal film through small interlayer openings.[6]

Technology has always driven a "smaller, faster, cheaper" ideology in the microelectronics industry. Aluminum was typically the most common metal used in the metallization process to deposit a conductive metal layer on the silicon wafer.[6] In August of 1997, IBM announced the first implementation of copper interconnect technology on integrated circuit

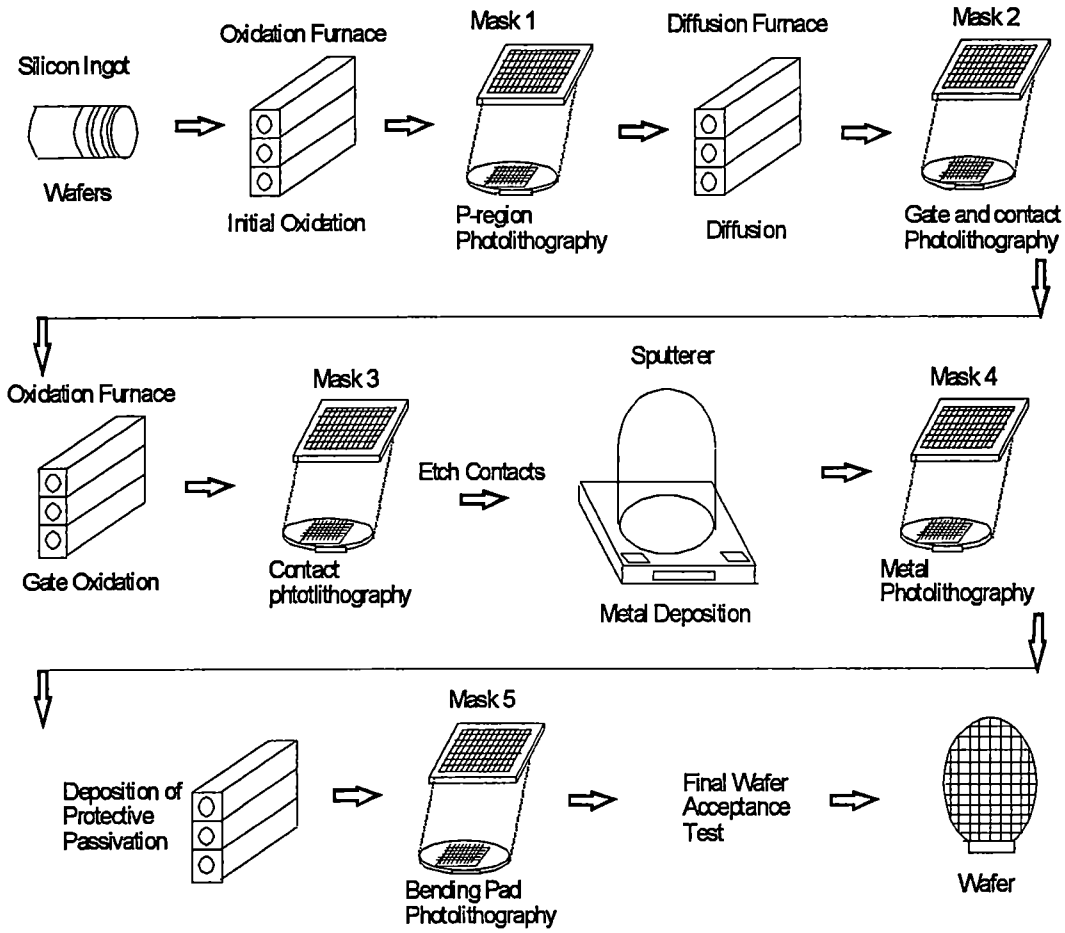

Figure 1.2. The steps involved in semiconductor fabrication.

Adapted from: Burgess, W. A. *Recognition of Health Hazards in Industry*; John Wiley and Sons: New York, 1995.

chips.[8] Copper offers many advantages relative to aluminum, including a lower resistance, higher allowed currentdensity, and increased scalability for chip wiring.[9] In addition, the process used to build a semiconductor with copper is 20-30% cheaper than the same process used to build with aluminum.[10] Copper electroplating of wafer interconnects still poses significant challenges due to the extreme requirements for uniformity, purity, and process control. Copper electroplating in the semiconductor industry is, however, becoming more popular.[11]

A new, near-neutral pH copper-plating electrolyte specifically for electroplating interconnects on silicon wafers was recently reported by Landau et al.[11] The elimination (or reduction) of the acid in this system was found to increase the electrolyte resistivity, which in turn decreased the detrimental effect of a thin seed layer on the uniformity of the deposit thickness. An enhancement of both the copper transport rate and copper solubility was also observed, providing fast, high quality copper deposition. This process also offers significant environmental and safety benefits since the solutions involved are in the neutral pH range.

1.1.3 Copper in Biological Systems and the Environment

Copper is essential to human life at low levels. Copper enzymes are involved in a variety of chemical processes within the body, including the utilization of oxygen during cell respiration, the synthesis of proteins of connective tissues of the skeleton and blood vessels, and in nervous tissue

function.[12] The human body contains around 80 mg of copper, and the healthy adult needs an intake of approximately 2 mg of copper per day. The main source of copper intake is the diet, although drinking water, dust, and copper cookware are also sources. Copper deficiency, known as Menke's disease, is rare and is associated with anemia, neutropenia (lowering of the white blood cells that fight infection), and bone abnormalities. Acute copper poisoning is also rare and usually results from contamination of food or beverages stored in copper containers or from the accidental or deliberate ingestion of copper salts. People with Wilson's disease, a condition leading to the progressive accumulation of copper, are at the highest risk for copper toxicity, with symptoms including stomach pain, nausea, hepatitis, liver cirrhosis, jaundice, and in extreme cases, death.[12]

Because high doses of copper affect the ecosystem and human health, and because it is so widely used, it is among the 13 toxic metal species on the Environmental Protection Agency's priority pollutant list and is regulated by the Resource Conservation and Recovery Act.[13] The Safe Drinking Water Act, passed by Congress in 1974, requires the EPA to determine safe levels of chemicals in drinking water, and the current Maximum Contaminant Level Goal for copper in drinking water is 1.3 parts per million.[14]

1.2 Chemical Sensing

The area of chemical sensing is of intense current interest; several journals specialize in chemical sensors, many universities offer graduate courses on the topic, professional societies have divisions devoted solely to sensors, and international conferences on sensor research are quite common. As of 1998, more than 2000 sensor-related papers were published each year,[15] and it has been estimated that this rate is growing at about 10% per year. In the past two decades, the area of chemical sensing has become an accepted component of analytical chemistry.[16]

A sensor is defined as any device capable of continuously and reversibly recording a physical parameter or the concentration of a chemical or biochemical species.[17] The "ideal" sensor does not exist; acceptable characteristics of a sensor are often a function of the application. However, all sensors have certain desirable characteristics in common, including:[18]

(a) *Signal output proportional to analyte concentration:* Although this is becoming less important with on-device electronics and processing options, the output of an ideal sensor should be directly proportional (or bear a simple mathematical relationship) to the amount of analyte species present in the sample.

(b) *Fast response time:* Real-time data is essential for on-line measurement. Long response times arising from slow kinetics can seriously limit the application range of sensors.

(c) *No hysteresis:* Although it is often ignored, hysteresis can be a major factor in analytical error. The signal from an ideal sensor should return to baseline after responding to the analyte.

(d) *Stability:* The indicating species within the sensor should not leach out or degrade over repeated measurements. Otherwise, the sensor must be re-calibrated often, increasing the cost and time for analysis.

(e) *Selectivity:* Selectivity refers to the degree to which the sensor is free from interference by species other than the analyte contained in the sample matrix. Without adequate selectivity, the signal obtained cannot be related to the target analyte with any confidence.

(f) *Sensitivity:* The ability to discriminate between small differences in analyte concentrations is essential. If the change in signal is large per unit change in concentration (i.e., the slope of the calibration curve is large), the sensor will be able to discriminate accurately between analytes of similar concentrations.

(g) *Limit of detection:* The detection limit is the minimum concentration of analyte that can be detected at a known confidence level. A good limit of detection is achieved by improving the signal-to-noise ratio, often by using the sensor in a flow analysis situation rather than for steady state measurements.

Most commonly, chemical sensing mechanisms are based on familiar optical or electrochemical methods. Optical techniques for chemical analysis are well established and include areas such as luminescence, absorption, and emission spectroscopy. Sensors based on optical methods are attracting considerable attention because of their applications in the environmental, medical, and industrial fields.[19] Chemical sensing based on optical methods has many attractive features when compared to other sensing types.[17,19,20] Numerous optical techniques are already developed for routine chemical analysis, and these techniques are non-destructive, making optical sensing ideal for small sample volumes. Low-loss optical fibers allow the transmittance of optical signals over large distances, enabling remote *in situ* monitoring of species in hard to reach or hazardous locations. Optical sensors may be miniaturized, allowing the development of small, portable sensors. Unlike electrochemical sensors, optical sensors do not require a reference signal and are not subject to electrical interferences by static electricity, magnetic fields, etc. Different reagents can be immobilized on a single sensor, allowing the simultaneous measurement of several analytes at one time. As with any method, optical sensing does have limitations, including interference from stray light, finite dynamic ranges, and limited long-term stability.

1.3 The Sol-Gel Process

The sol-gel process refers to a series of reactions involving a variety of alkoxide precursors to prepare inorganic materials such as glasses and ceramic oxides.[21] Sol-gel materials are stable thermally, chemically, and mechanically, and are completely transparent in the visible and near UV regions, making them excellent candidates for optical sensors.[22] Sol-gel materials are inexpensive and simple to prepare. The characteristics of the sol-gel glass product can be tailored by varying a number of factors, including the precursor and solvent chosen, the solution pH, the drying time or temperature, and the presence of catalysts or chemical additives. The versatility of these materials has led to their use in a variety of forms, including thin films and protective coatings, optical fibers and components, powders, beads, and membranes.[21]

Because bulk sol-gel materials are not suitable for optical analysis, sol-gel monoliths were used in the current study. The preparation of a sol-gel monolith generally involves five distinct steps: mixing, casting, gelation, aging, and drying.[23] During the mixing step of the sol-gel process, a liquid alkoxide precursor, such as tetramethyl orthosilicate (TMOS), is hydrolyzed by mixing with water. The silanol groups then interact in a condensation reaction forming –Si-O-Si- bonds; this condensation continues, eventually resulting in a SiO_2 network. The water and alcohol expelled from the reaction remain in the pores of the network. This series of reactions is

shown in **Figure 1.3**. Catalysts can strongly influence both the hydrolysis and condensation rates, as well as the properties of the final glass product.

In the acid-catalyzed sol-gel reaction, as shown in **Figure 1.4**, rapid dissociation of either the –HOR or –HOH substituents bonded to Si occurs, leading to slower hydrolysis and faster condensation in acid catalyzed gels. The gelation time is slow, and the resulting gels are highly dense with a low pore volume and small pore size. Under basic conditions, the hydroxyl OH^- ions attack Si directly as shown in **Figure 1.5**, causing faster hydrolysis and slower condensation reactions.[24] Gelation is fast, and the resulting low-density gels have a high pore volume and large pore size. Metal ions can easily diffuse into the gels, offering the advantage of fast kinetics, an essential property for a sensor. Thus, base catalyzed gels were used throughout these studies.

The product formed after mixing is a low-viscosity liquid, or sol, that may be cast into a mold; this mold must be carefully selected to avoid adhesion of the gel. The hydrolysis and condensation reactions lead to the growth of clusters that eventually contact and link together to become a three-dimensional gel network. The physical characteristics of this gel network depend on the size of the particles and the extent of cross-linking in the early stages of the sol-gel process. At the gelation point, the viscosity increases sharply, and a solid object results in the shape of the mold used for casting. Aging involves maintaining the solid gel for a period of time immersed in liquid. Polycondensation continues during aging, thus

Hydrolysis



Condensation

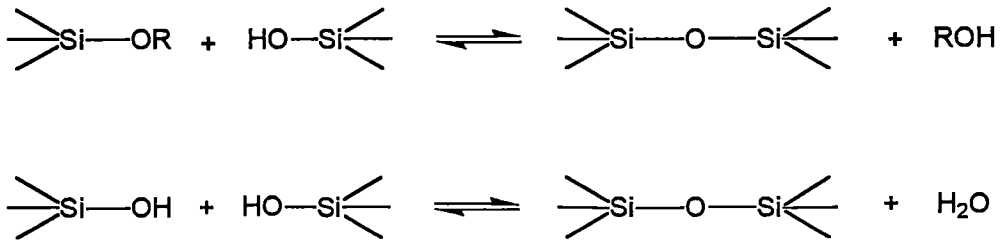

Figure 1.3. The sol-gel reactions.

Acid-Catalyzed Hydrolysis:

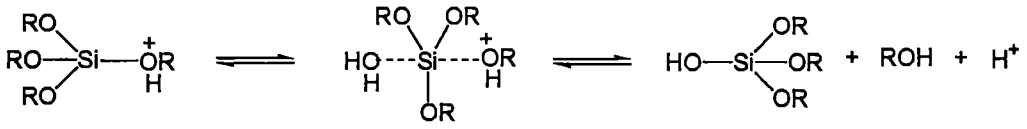

Acid-Catalyzed Condensation:

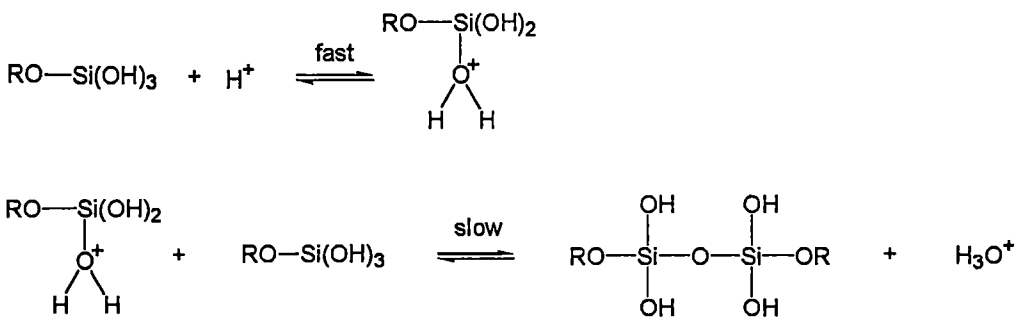

Figure 1.4. The acid-catalyzed mechanism in the sol-gel process.

Adapted From: Buckley, A. M.; Greenblat, M. *J. Chem. Educ.* **1994**, *71*, 599-602.

Base-Catalyzed Hydrolysis:

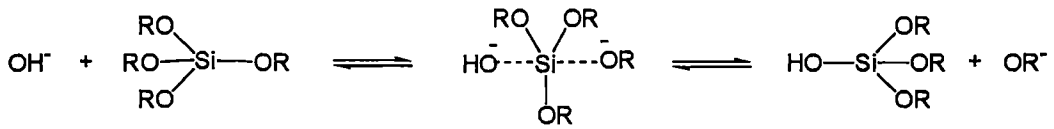

Base-Catalyzed Condensation:

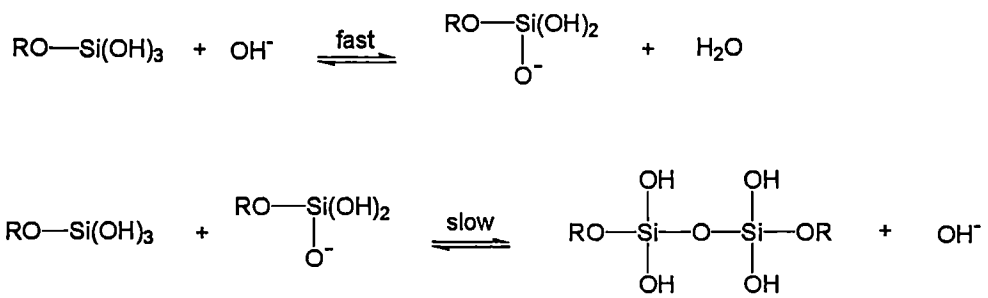

Figure 1.5. The base-catalyzed mechanism in the sol-gel process.

Adapted From: Buckley, A. M.; Greenblat, M. *J. Chem. Educ.* **1994**, *71*, 599-602.

increasing the strength of the gel. Aging is critical, since an aged gel must develop sufficient strength to resist cracking during drying. During the drying step, the liquid is removed from the interconnected pore network within the gel. Large capillary stresses can develop during this stage due to pressure gradients within the gel structure, causing the gel to crack. This cracking may be prevented either by slow evaporation of the liquid within the gel pores or by the addition of drying control chemical additives. If the gel is dried under ambient conditions, a xerogel results, which often shrinks to about one-eighth the original pore volume of the wet gel. If drying is carried out in an autoclave under supercritical conditions, the resulting gel is called an aerogel, since it is composed mostly of air and has the volume fraction of solid as low as ~1%.[21] Xerogels were used in the current studies.

Since little or no heating is required in the sol-gel process, it is possible to encapsulate thermally sensitive organic molecules into the interior of the gel. Two techniques are used to achieve this encapsulation: doping and grafting. In the doping process, the desired dopant is added to the solution before polymerization (gelation) occurs and the glass preparation is stopped at the xerogel stage.[20,22,25] This technique is simple and may be applied to a variety of organic molecules. However, the pore size must be carefully tailored to the size of the dopant to entrap it within the structure of the gel. Depending on how well tailored the pores are, leaching of the dopant molecule is often a problem. The grafting technique is more

complicated than the doping technique because the molecules encapsulated within the gel must contain a functional group compatible with covalent bonding.[26] This technique is advantageous over the doping technique because the indicating species is covalently bound to the gel and leaching is not a problem.

The ligands used in this study, 3-aminopropyltrimethoxysilane (monoamine) and N-[3-(trimethoxysilyl)propyl]ethylenediamine (diamine), are shown in **Figure 1.6**. These ligands were carefully selected to provide two essential properties. First, each ligand had to contain a group that could be covalently bound to the surface of a porous silica sol-gel. In the presence of water, the $(MeO)_3Si$- group on one end of the ligand participates in the reactions of the sol-gel process to form silanol groups on the surface of the monolith, covalently tethering the ligand to the surface of the gel. Second, the ligands had to contain a functional group capable of binding Cu^{2+} ions and forming a colored complex that could be observed by UV/visible spectrophotometry. Because the chemistry of the copper:ammonia complex $Cu(NH_3)_n^{2+}$ is well known, the ligands chosen for this study contained an $-NH_2$ functional group.

1.4 Ultraviolet/Visible Absorption Spectrometry

Spectroscopy is the study of the interaction of electromagnetic radiation with matter. When a molecule absorbs energy from light in the form of a photon, the energy of that molecule is increased. Electromagnetic

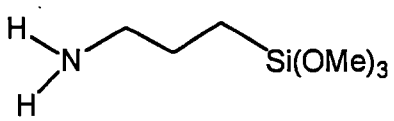

3-aminopropyltrimethoxysilane (monoamine)

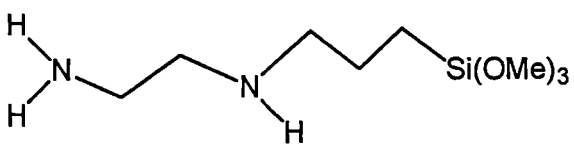

N-[3-(Trimethoxysilyl)propyl]ethylenediamine (TMSen)

Figure 1.6. Bifunctionalized amine ligands chosen as the sensing element on a solid state sol-gel support.

radiation in the form of ultraviolet or visible light is energetic enough to promote the outer electrons of molecules to higher energy levels, giving rise to certain spectral characteristics. In spectrophotometry, the transmission of light through a solution is used to determine the concentration of an analyte within the solution.[27]

A spectrophotometer, as shown in **Figure 1.7**, has four major components: a radiation source, a wavelength selector, a sample compartment, and a detector:

(a) *Radiation source*: The source supplies the energy for absorption by the analyte molecule, and a good source should contain energies of sufficient intensity in the region where the analytes of interest absorb. Perhaps the most common radiation source for visible radiation is the tungsten/halogen lamp.[28] Typically, these lamps produce radiation from 320-2500 nm, covering the entire visible region and parts of the IR and UV regions as well.

(b) *Wavelength selector*: A monochromator is used to select a particular wavelength of radiation for use in analysis. Most commonly, a grating is used to disperse light into its component wavelengths. In a grating monochromator, shown in **Figure 1.8**, polychromatic radiation enters through a slit and strikes a concave mirror, where it is collimated into a beam of parallel rays. These rays fall on a reflection grating, where different

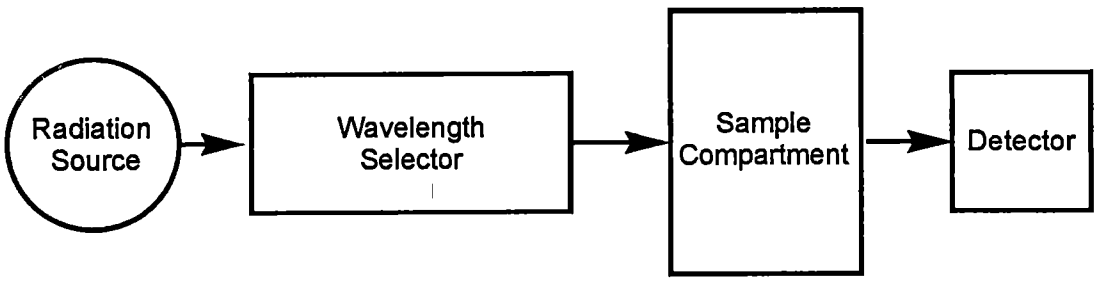

Figure 1.7. A typical single-beam spectrophotometer.

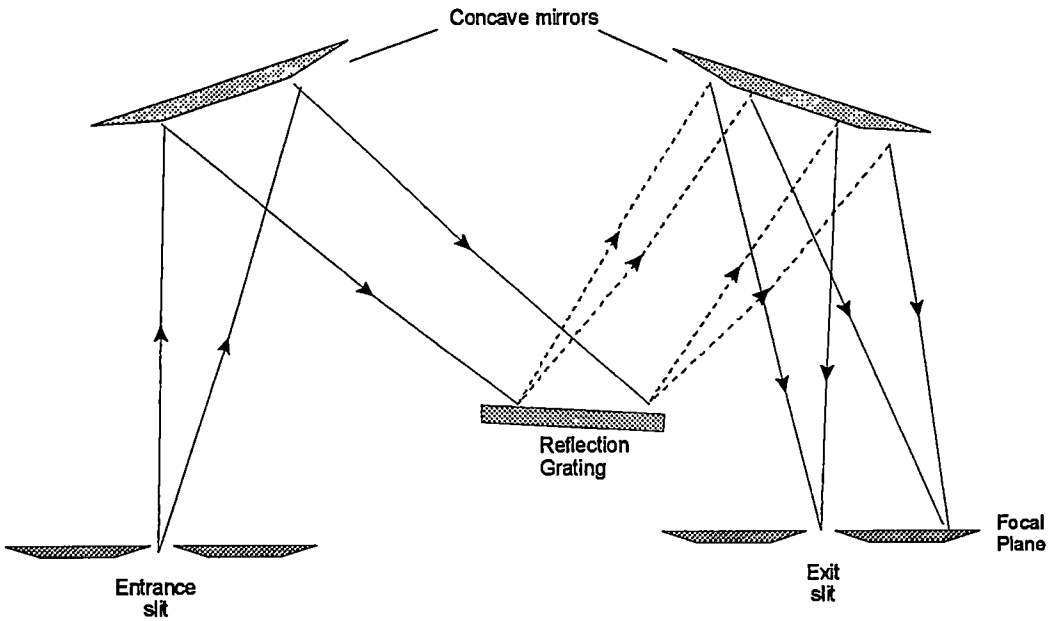

Figure 1.8. Diagram of a Czerny-Turner grating monochromator.

Adapted From: Harris, D. C. *Quantitative Chemical Analysis*; 4th ed.; W. H. Freeman and Company: New York, 1995.

wavelengths of light are diffracted at different angles. The light then strikes a second mirror, which focuses each wavelength at a different point. Only one narrow band of wavelengths is allowed to reach the sample through an exit slit.[27]

(c) *Sample compartment*: These come in various sizes and shapes that are unique to particular experiments. The most important characteristic of a sample cell is that it must be constructed of a material that does not absorb radiation in the spectral region of interest.

(d) *Detector*: The detector converts radiant energy from photons into an electrical signal. One of the more sensitive detectors is a charge-coupled device (CCD), shown in **Figure 1.9**, which is composed of an array of holes called potential wells. When a photon strikes the CCD, it releases an electron from the silicon lattice, which then falls into one of the potential wells where it is trapped. The first pixel in a channel of the CCD is read, and then all the channels are shifted up by one pixel and the next row is read. The CCD is sensitive due to its high quantum efficiency and low background noise.[27]

Optical fibers are commonly used in spectroscopic analysis, although they are usually not essential components of spectrophotometric instruments. A typical optical fiber (**Figure 1.10**) consists of a core with

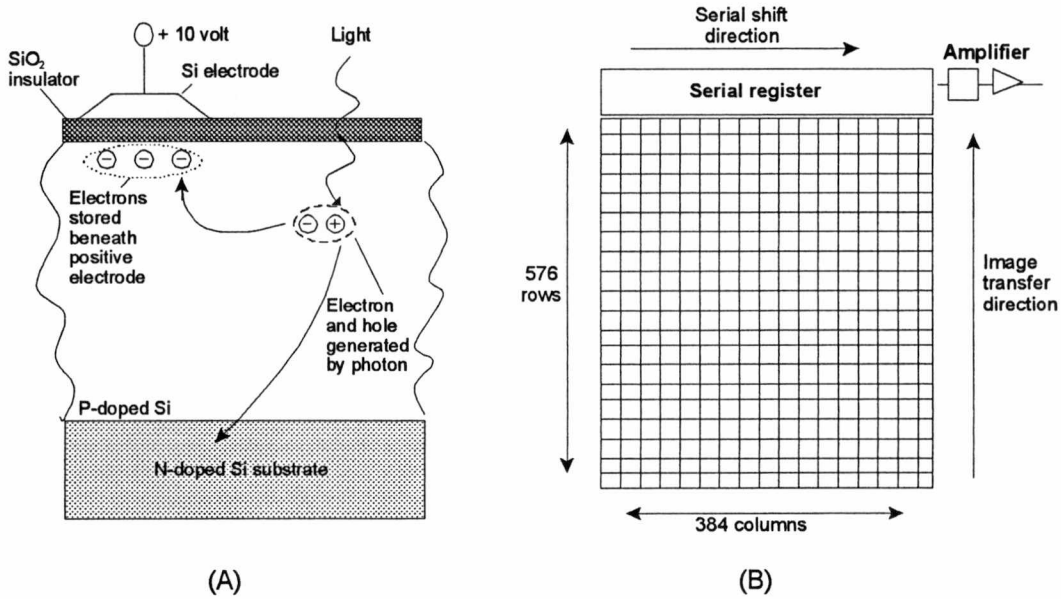

Figure 1.9. Schematic representation of a charge coupled device (CCD). (a) Cross-sectional view indicating charge generation and storage in each pixel. (b) Top view showing two-dimensional nature of one particular array.

Adapted From: Harris, D. C. *Quantitative Chemical Analysis*; 4th ed.; W. H. Freeman and Company: New York, 1995.

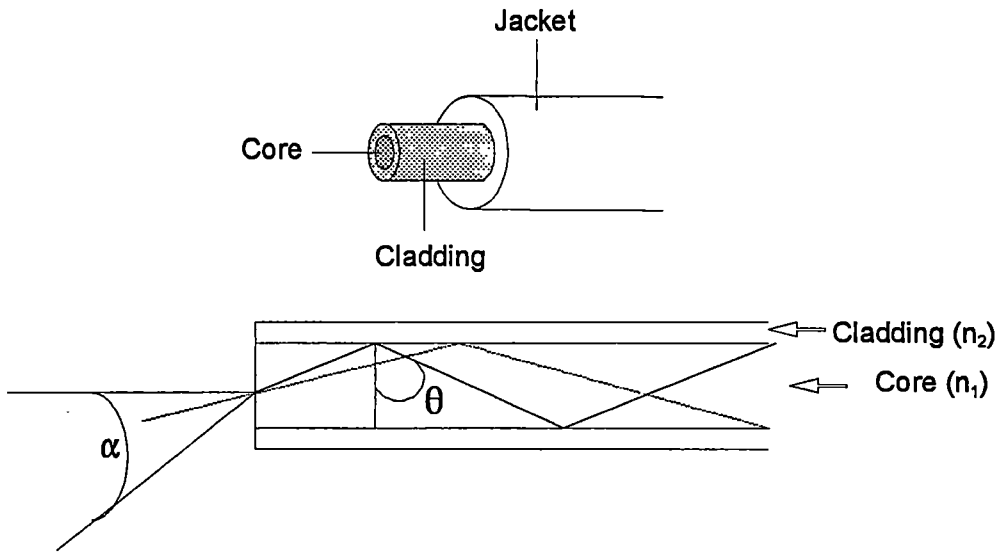

Figure 1.10. Top: Schematic of an optical fiber. Bottom: Path of light in a waveguide. α is the acceptable angle; n_1 and n_2 are the refractive indicies for core and cladding; θ is the critical angle for total reflection to occur.

Adapted from: Wolfbeis, O. S. In *Fiber Optic Chemical Sensors and Biosensors*; Wolfbeis, O. S., Ed.; CRC Press: Boca Raton, 1991; Vol. 1, pp 1-23.

refractive index n_1 surrounded by a cladding with lower refractive index n_2. Light is guided in the fiber with very low intensity loss by a series of total internal reflections at the core-cladding interface.[17,19] Fiber optic technology has been optimized by the communications industry, and optical fibers allow the transmission of light over large distances at relatively low cost.

In the experiments in this study, an Ocean Optics Instruments S2000 miniature fiber optic spectrometer with a Sony ILX511 linear CCD-array silicon detector was used. An Ocean Optics LS-1 tungsten-halogen lamp was used as the light source. The sample compartment was specially designed and fabricated from chemically-resistant Teflon materials. It holds the sol-gel sensors steady in flowing metal ion solutions, and supports two optical fibers through optically transparent cylindrical glass tubes that are used to isolate the fibers from the solution. Silica-core, silica-clad optical fibers connecting the source, sample flow cell, and detector were purchased from Ocean Optics. The spectrometer was interfaced to a personal computer using the ADC500 ISA-bus A/D card, and Ocean Optics OOIBase32 spectrometer operating software was used to set experimental parameters and collect data. The sample compartment was connected to the metal ion solutions and to a Barnant Company variable flow diaphragmatic pump through Teflon tubing. The instrument design is shown in **Figure 1.11**. This system provides a low-cost and portable spectrometer suitable for field sensor applications.

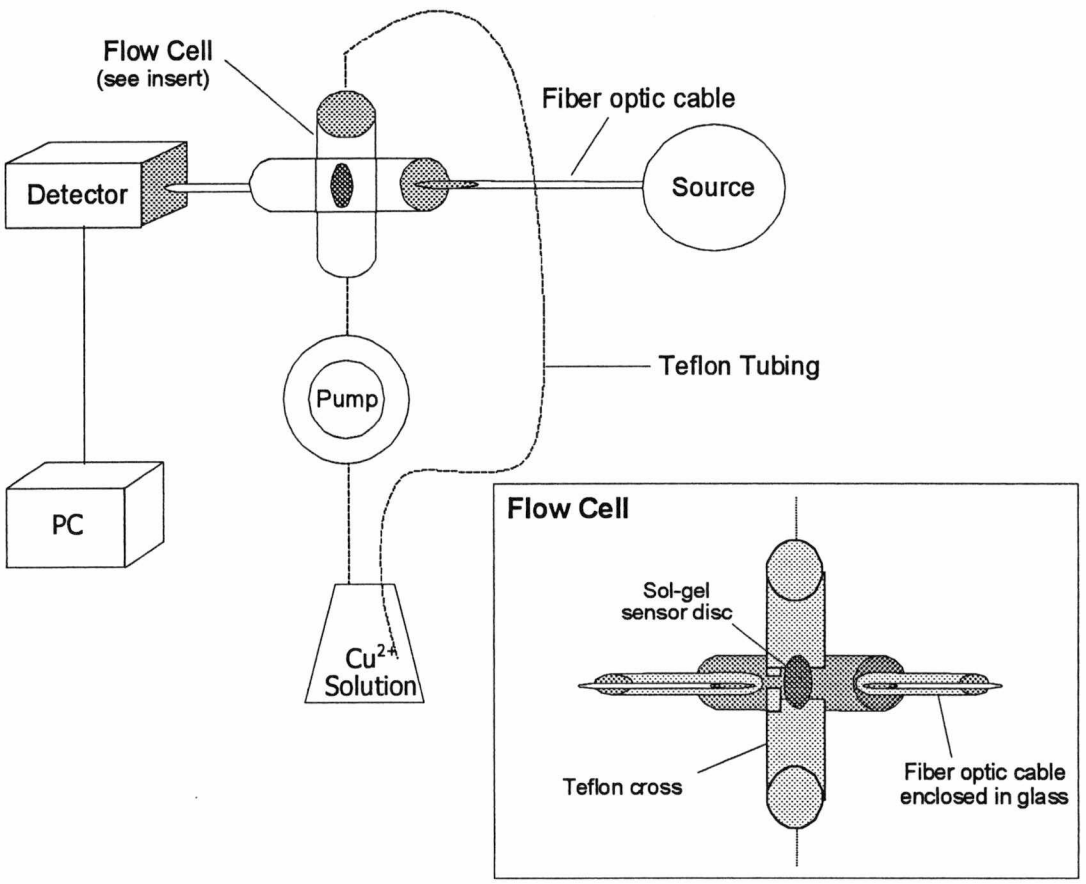

Figure 1.11. Instrumental design used in the current studies.
Inset: Magnification of the flow cell/sensor holder.

One of the most important concepts in spectrophotometry is the Beer-Lambert law, more commonly referred to simply as Beer's law:[27]

$$A = log\ (P_0/P) \qquad \text{(Eq. 1.1)}$$

where A = the absorbance measured by the spectrophotometer, P_0 = the radiant power of the light striking the sample, and P = the power from the beam emerging from the other side of the sample. Beer's law may also be expressed as:

$$A = \epsilon bc \qquad \text{(Eq. 1.2)}$$

where ϵ = the molar absorbtivity of the absorbing species (the analyte's intrinsic ability to absorb light, characteristic of a particular substance) in M^{-1} cm^{-1}, b = the pathlength in cm, and c = the molar concentration of the absorbing species. Beer's law shows that the absorbance of a sample is directly proportional to the concentration of light-absorbing species within the sample. Although Beer's law is widely applicable in most cases, it does have some limitations. At high concentrations (usually > 0.01 M), analyte molecules begin to influence one another as a result of their close proximity. When molecules interact, their properties change, and the relationship between absorbance and concentration is no longer linear. Chemical

deviations from Beer's law can arise when analyte molecules dissociate or react with solvent molecules, as often seen with acid/base indicators.[28]

Metal ions often show broad absorption bands in the visible range, and these bands are strongly influenced by chemical environmental factors. For example, Cu^{2+} is pale blue in aqueous solution, whereas its ammonia complexes $Cu(NH_3)_n^{2+}$ are much darker blue in color. The spectral characteristics of Cu^{2+} involve electronic transitions among energy levels of the d-orbitals. Perhaps the simplest theory to explain the colors of transition metal ions and the influence of chemical environment on these colors is the crystal field theory.[28] Energies of d-orbitals in complexes are not degenerate, as they are in the metal ions in the gas phase. When a complex forms between a metal ion and a ligand, splitting of the d-orbital energies results. Absorption involves the transition of electrons from a lower-energy d-orbital to a higher-energy d-orbital. The splittings depend on a number of factors, including the oxidation state of the metal, the number and geometry of surrounding ligands, and the nature of the ligands themselves.[29,30]

1.5 Brunauer-Emmett-Teller Gas Adsorption Analysis

The Brunauer-Emmett-Teller (BET) gas adsorption technique is commonly used to measure the specific surface area, pore volume, and pore size distribution of solid materials. A BET gas adsorption analyzer consists of a gas storage system, a gas dosing system, a pressure-

measuring device, and a sample unit to which the gas is to be delivered. In this research, BET analysis was conducted using the Quantachrome Corporation Nova 1000 Gas Sorption Analyzer. The dry sample to be analyzed is evacuated of all gas and cooled to 77 K using liquid nitrogen. At this low temperature, inert gasses such as nitrogen will physically adsorb on the surface of the sample. As more gas molecules are introduced into the system, the adsorbate molecules form a thin layer that covers the adsorbent surface. If a known amount of gas is added to the sample system, the amount that is unadsorbed may be determined by applying the gas laws.[31] The determination of the surface area of the solid material involves the use of the BET equation as follows:[32]

$$1 / W[(P_0/P)-1] = 1 / W_m C + ((C-1) / W_m C) * (P/P_0) \qquad \text{(Eq. 1.3)}$$

where W is the weight of gas adsorbed at a relative pressure P/P_0, and W_m is the weight of adsorbate making up a monolayer of surface coverage. The C term is the BET constant, which is related to the energy of adsorption in the first adsorbed layer, and its value indicates the magnitude of the adsorbent/adsorbate interactions.

A plot of $1 / W[(P_0/P)-1]$ versus P/P_0 is linear in a multipoint BET. This plot is restricted to a small range of relative pressures (P/P_0 from 0.05 to 0.35) and requires a minimum of three points in this range. The slope (s)

and intercept (*i*) of the BET plot can then be used to obtain the weight of a monolayer of adsorbate W_m by the following equation:[33]

$$W_m = 1/(s+i) \qquad \text{(Eq. 1.4)}$$

Once the weight of adsorbate is known, the total surface area, S_t, can then be calculated by the following:[32]

$$S_t = (W_m N A_{cs})/M \qquad \text{(Eq. 1.5)}$$

where N is Avogadro's number (6.023×10^{23} molecules/mole), M is the molecular weight of the adsorbate, and for a hexagonal close-packed nitrogen monolayer at 77 K, the cross sectional area, A_{cs}, is 16.2 $Å^2$. The specific surface area can then easily be calculated by dividing the total surface area by the sample weight.

The pore size within a material is a real observation that can aid in sample characterization. Pores with diameters smaller than 20 Å are called micropores, while those with diameters larger than 500 Å are called macropores. Pores that fall between this range of 20-500 Å are referred to as mesopores.[34] However, the size of a pore opening alone does not adequately describe the porosity of solid materials. Total pore volume and the pore size distribution are often more important in characterization.

The total pore volume can be described as the amount of vapor adsorbed at a relative pressure $P/P_0 \approx 1$. At this relative pressure, the assumption is made that the pores are filled with liquid adsorbate. The volume of nitrogen adsorbed, V_{ads}, can be converted to the volume of liquid nitrogen, V_{liq}, contained in the pores using the following equation:[32]

$$V_{liq} = (P_a V_{ads} V_m) / RT \qquad \text{(Eq. 1.6)}$$

where P_a is ambient pressure, T is ambient temperature, and V_m is the molar volume of the liquid adsorbate (34.7 cm^3/mol for nitrogen). The average pore size can then be estimated by assuming cylindrical pore geometry and using the following equation:[32]

$$r_p = 2V_{liq} / S \qquad \text{(Eq. 1.7)}$$

where V_{liq} is again the volume of liquid nitrogen contained in the pores and S is the surface area.

The pore size distribution is simply the distribution of pore volume with respect to pore size. The pore size distribution is important because it is a measure of the uniformity of the pores throughout the material and it indicates the sizes of the pores that constitute the majority of the pore volume. On a plot of pore volume (in cc/g) versus pore diameter (in Å), a narrow pore size distribution is represented by a sharp peak, indicating that

the pores within the solid are uniform in size throughout the bulk of the material.

1.6 Scanning Electron Microscopy

Scanning electron microscopy (SEM) is an imaging technique capable of producing high-resolution images at high magnification. A diagram of an SEM instrument is shown in **Figure 1.12**. The electron gun produces a beam of electrons that is focused through condenser and objective lenses onto a fine point on the sample. The scan coils, located within the objective lens, are energized by a varying voltage and create a magnetic field that deflects the beam of electrons in a controlled pattern. This voltage is also applied to a set of deflection coils around the neck of a cathode-ray tube (CRT), and the magnetic field from these coils causes the deflection of a spot of light back and forth on the surface of the CRT. The primary electrons in the beam strike the sample in a constant scanning motion, causing the ejection of secondary electrons, which carry information about the surface structure of the sample. These secondary electrons are collected by a detector, processed, and then reassembled in their original configuration on the CRT. The deflection pattern of the beam of electrons on the sample is the same as the deflection pattern of the spot of light on the CRT. The CRT, which is similar to a television set, displays a picture of the sample surface that changes continuously as different parts of the sample are placed in the electron beam.[35] In the current studies, the Hitachi S-4700

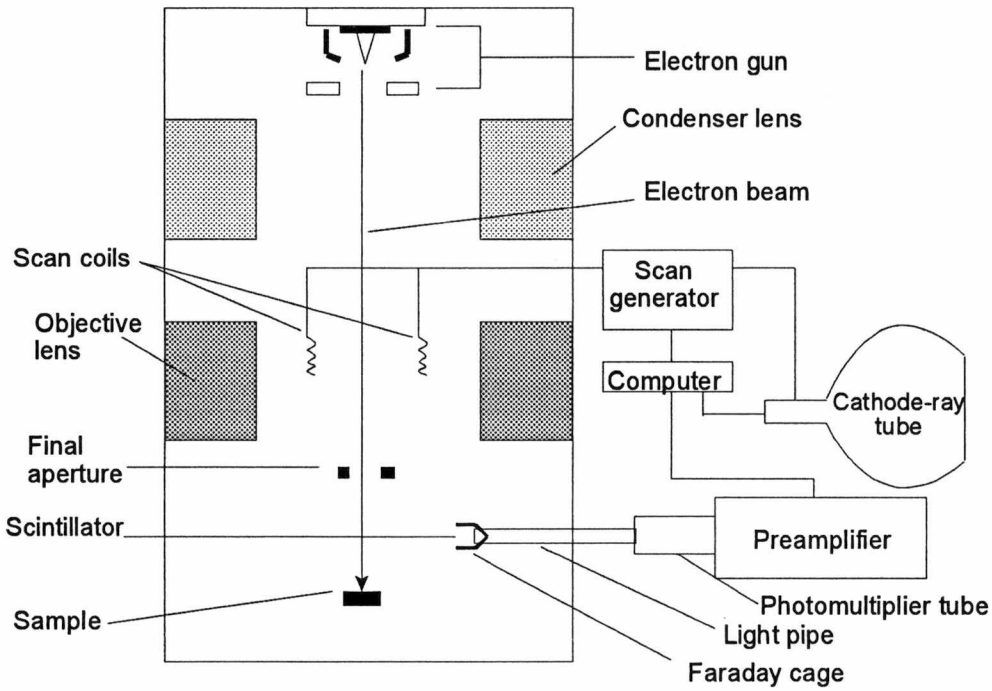

Figure 1.12. Schematic of a scanning electron microscope.

Adapted From: Flegler, S. L.; John W. Heckman, J.; Klomparens, K. L. *Scanning and Transmission Electron Microscopy: An Introduction*; W. H. Freeman and Company: New York, 1993.

FEG-SEM was used for scanning electron microscopy analysis, and this analysis was conducted by John W. Clavier at Oak Ridge National Laboratory.

Because electron microscopes use an electron beam to form a magnified image of the object under investigation, they offer several advantages over conventional optical microscopes. In a traditional light microscope, photons are used to form images and because photons are large (in the context of subatomic particles), the amount of available magnification is limited to only several thousand times the size of the photon, between 10-1000X the size of the object being magnified. In addition, only one level of the sample may be focused at one time, so if the object under the lens is three-dimensional, part of it will always be out of focus. The scanning electron microscope solves the problems of limited magnification and depth of field. Electrons are much smaller than protons, and so they can provide a much greater resolving power. With SEM, it is possible to achieve magnifications in excess of 300,000X, although the typical working range is 20-100,000X.[36] Electrons are abundant and easily manipulated, and by moving the sample and changing the focus, magnification, and beam parameters of the instrument, a clear three-dimensional image may be achieved.[37]

1.7 Overview of this Thesis

The objective of the work described in this thesis is to develop an optical ion sensor through the sol-gel process for the determination of heavy metal ions, such as Cu^{2+}, in flowing solutions. The development of a sol-gel monolith grafted with a diamine ligand as a single-use probe for Cu^{2+} is described in Chapter 2, as well as the difficulties of the sol-gel processing of inorganic/organic hybrid materials. Chapter 3 describes the successful development of a reversible Cu^{2+} sensor based on sol-gel materials grafted with a monoamine ligand using a molecular imprinting approach. Both the probe described in Chapter 2 and the sensor illustrated in Chapter 3 allow a fast response to Cu^{2+}, and the visible absorbance spectra of the complexes formed within these sol-gel monoliths is easily correlated to $[Cu^{2+}]$. The approaches outlined in this thesis offer a simple, fast, and economical route to Cu^{2+} determination for both industrial and environmental applications.

CHAPTER TWO

PHYSICALLY ROBUST, OPTICALLY TRANSPARENT SOL-GEL MONOLITHS GRAFTED WITH DIAMINE LIGANDS FOR SINGLE-USE COPPER (II) DETERMINATION

2.1 Introduction

Environmental awareness has grown within the past few decades in part because of detailed research into the behavior and effects of trace metals in various ecosystems. Copper is essential to our health and our lifestyles, and this metal plays a vital role in the areas of engineering, science, agriculture, art, medicine, and architecture.[38] As part of the group of oxidizing enzymes, low levels of copper are essential to the healthy life of many plants and animals, including humans. However, copper can be toxic in large quantities, especially to the lower members of the human food chain. Because this metal is so widely used and because it is potentially toxic, copper in the environment, particularly in water supplies, is strictly regulated by the Environmental Protection Agency.[13,14,39] The most common means for the determination of aqueous copper is atomic absorption analysis, but this technique often requires a preconcentration step and the instrumentation used prohibits on-site field-testing.[40] For a more cost-effective means of the determination of copper in environmental

field applications, the development of a fast, reliable metal ion probe or sensor is desirable.

It is important to understand the difference between a probe and a sensor. A heavy metal ion sensor is a device capable of selectively measuring small changes in metal ion concentrations and is fully reversible. A probe, however, may or may not respond selectively to a particular metal ion and can only be used one time for concentration measurements before it must be disposed. Frequently, the sensing mechanism of a probe is based on reactions between the target metal ion of interest and a chelator with more than one bonding site for the target ion. The chelating reactions must be reversible in principle to allow the release of the metal ion from the chelator. In practice, however, the release of the metal ion from the chelator is often difficult for two important reasons.[41] First, the formation stability constant between the metal ion and the chelator is often very large and the binding between the two ions is fast. Further increase in metal ion concentration produces little or no change in the observed signal.[41b] The second problem in terms of sensor reversibility is the strong binding between the chelator and the metal ion makes the release of the metal ion thermodynamically unfavorable, and often requires harsh chemical additives. Given these difficulties, and the fact that probes are usually simple and inexpensive to prepare, single use probes have become increasingly common and in some cases may even be more desirable than chemical sensors. In environmental field applications, single-use probes are

commonly used because they offer a fast, cost-effective means of gathering chemical information. Even probes that display little or no specificity can be desirable for rapid screening purposes where a sample only needs to be further analyzed by more expensive methods if it gives a positive test for metal ions of interest.[41a]

Literature reports of heavy metal ion probes based on optical methods are common.[41-47] Optical probes with immobilized fluorophores for Cd^{2+} and Fe^{3+} as well as for Cu^{2+}, Co^{2+}, and Ni^{2+} have been reported.[42,43] The fluorescence intensity of the immobilized fluorophores was found to either increase[42] or decrease[43] as a function of the addition of metal ions. The binding constant between the reagent and the metal ions may be extremely large, and the reagent completely extracts metal ions from solution.[43] In such a case, the method has been more commonly used as a preconcentrating reagent or a reusable titration end-point indicator. A simple cuvette test for the determination of heavy metal ions has also been described.[44] In this method, a cuvette containing urease was coated with an ammonia-sensitive layer, and the addition of heavy metal ions was found to inhibit the formation of ammonia. Although this probe responded to part-per-billion concentrations of heavy metal ions and could be manufactured in bulk at low cost, its usefulness is limited in that the time for each analysis is approximately 20 min and the indicator leaches out over time. Probes specific for copper (II) ion have also been reported. A lipophilic 8-hydroxyquinoline derivative was dissolved in plasticized poly(vinyl chloride)

(PVC) and upon the addition of Cu^{2+}, the absorbance at 580 nm increased due to deprotonation and complexation with Cu^{2+} ions.[45] This probe was effective in determining the concentration of Cu^{2+} from 1-100 μM within 2 min. However, only four different Cu^{2+} concentrations were studied, and the system could only detect Cu^{2+} in acidic environments (pH 2.5). In addition, the reagent must be synthesized, increasing the time and cost of analysis. Cu^{2+} determination has also been carried out in the 0.15-43 μM range by dissolving bathocuproine in a plasticized PVC membrane and measuring the absorbance of the Cu^{+}:bathocuproine complex at 480 nm.[46] However, Cu(II) must first be reduced to Cu(I), and the measurements fluctuate with changes in temperature and pH. Wolfbeis and coworkers developed a method for the determination of Cu^{2+} that involved the immobilization of a Zincon-tetraoctyl-ammonium ion pair within a polyester support membrane.[47] The addition of Cu^{2+} to the membrane and the formation of a Cu^{2+}:zincon complex produces a color change from pink to blue, and the absorbance of this color change was measured at 620 nm. The probe was pH dependent, and high concentrations of cobalt or nickel ions resulted in large errors. The potential large-scale use of the membrane is limited by the ~10% error in measurements from different probes prepared in the same manner.

Bulk sol-gel materials grafted with ligands have been used as metal ion sorbents and in chromatographic applications.[48-51] However, there have been few reports of optical determination of transition metal ions by

functionalized sol-gel monoliths. Sol-gel processing is a delicate balance of a number of experimental variables, including the nature and ratios of starting materials, pH, temperature, and aging and drying times. Creating a purely inorganic sol-gel monolith is quite common,[21,23] but the incorporation of organic ligands into the sol-gel matrix makes the development of a mechanically stable monolith of good optical quality much more difficult due to the numerous experimental parameters that must be carefully controlled.

A method is reported here for the preparation of physically robust, crack-free sol-gel monoliths containing an ethylenediamine derivative for Cu^{2+} determination. A ligand-grafting approach was employed to covalently bond the bidentate ligand to the gel interior. A correlation between the change in the absorbance of the Cu^{2+}:ligand complex within the gel vs. time and $[Cu^{2+}]$ was observed, and the $[Cu^{2+}]$ in flowing aqueous solutions could be determined. Cu^{2+} removal from the amine ligand within the monolith with HCl was possible, but subsequent neutralization of the monolith with base was unsuccessful, and thus these probes were for single-use only.

2.2 Experimental Section

The chemicals used in this study, including $CuCl_2 \cdot 2H_2O$ (Mallinckrodt, analytical reagent), $NH_2(CH_2)_2NH\text{-}(CH_2)_3Si(OCH_3)_3$ (N-[3-(trimethoxy silyl)propyl]ethylenediamine (TMSen), Aldrich, 97%), $Si(OMe)_4$ (TMOS, Aldrich, 98%), CH_3OH (MeOH, Mallinckrodt, 99.9%), $CH_3(CH_2)_{15}N(CH_3)_3Br$ (CTAB, Aldrich), and $HO\text{-}CH_2CH_2\text{-}OH$ (Fisher, Certified), were used as

received. Ultra-pure deionized water was used in the preparation of all gels and aqueous $CuCl_2$ solutions. Distilled water was used in gel washing. Unless otherwise noted, UV/visible spectrophotometry was performed using an Ocean Optics S2000 miniature fiber optic spectrophotometer interfaced to a flow-cell designed to hold the sol-gel monoliths steady in flowing solution while supporting two fiber optic cables that connected the source, sample, and detector. Data was collected using Ocean Optics OOIBase32 operating software. Gels used in these experiments were prepared in bulk; the following procedures are for the preparation of a single gel. Amounts of reagents were increased stoichiometrically to give the desired number of gels. All of the sol-gel monoliths were stored in deionized water before use. $CuCl_2$ solutions ranging in concentration from 5.00-99.98 mM were prepared gravimetrically using ultra-pure deionized water as the solvent. Attempts were initially made to buffer these solutions in the pH 5.0-7.0 range; however, precipitation of Cu^{2+} with the buffer anion was found at high Cu^{2+} concentrations in these studies. The $CuCl_2$ solutions used in these experiments were thus not buffered.

2.2.1 Unsuccessful Attempts to Prepare a Stable Sol-Gel Monolith

Sol-gel processing is often considered to be as much of an art form as it is a science. Several experimental variables effect the outcome of the final inorganic glass product, and the preparation of a physically strong, optically transparent sol-gel disc with organic ligands incorporated directly

into the matrix proved to be challenging. The gels described here, for reasons discussed below, could not be used experimentally for the determination of [Cu^{2+}]. However, their preparation ultimately led to the development of a solid sol-gel disc that could be used as a Cu^{2+} probe, and it is therefore important to present a description of some of these failed attempts at creating a high quality solid monolith.

2.2.1.a Spin-Coating Sols onto Glass Slides (*Gel Series 2-A*)

TMSen (70 µL, 0.321 mmol), TMOS (595 µL, 4.03 mmol), and MeOH (300 µL, 7.41 mmol) were combined, with stirring, in a glass vial. To this vial, 300 µL of either H_2O, 0.5-2.0 M HCl, or 0.60 M NH_4OH (several different concentrations of catalysts were attempted in the preparation of different gels) was added. When the solution began to increase in viscosity, it was coated onto a glass microscope slide by a spin coating process (1650 rpm). The sol-gel film was dried in air for 3 days and then heated at 40 °C for seven days. None of the *gel series 2-A* was used in further analysis because the coated slides obtained by this method were of poor physical or optical quality. When these slides were placed in a $CuCl_2$ solution, no observable color change was seen on the slide. This suggested that either the pores of the sol-gel film were not large enough to allow the diffusion of sufficient Cu^{2+} ions into the gel interior, or the amount of ligand coated onto the slide was too small to produce an observable quantity of the colored Cu^{2+}:amine complex. The molar absorbtivity coefficient of Cu^{2+}:amine

complexes is quite low, and therefore according to Beer's Law ($A = \epsilon bc$), the pathlength (b) may have to be increased to compensate for the low absorbtivity (ϵ).

2.2.1.b Preparation of Monoliths in Cuvettes (*Gel Series 2-B*)

To increase the thickness of the sol-gels, an attempt was made to prepare the gels in a 1 cm cuvette. In the simplest starting mixture, TMSen (55 µL, 0.252 mmol), TMOS (470 µL, 3.19 mmol) and MeOH (470 µL, 11.60 mmol) were combined, with stirring, in a glass vial and then transferred to a polystyrene cuvette. H_2O (47 µL-60 µL) was then added to the solution. The cuvette was capped, shaken vigorously to mix its contents, and placed on its side on the laboratory bench. Gelation began almost instantly upon the addition of water. Initially, colorless gels formed in each of the cuvettes, but these gels cracked into dust-like pieces within 24 h.

Using the same ratios of starting materials, more gels were prepared and then dried under different conditions: at room temperature, in the fume hood, in the oven at temperatures ranging from 40 °C-100 °C. Some of these gels were capped tightly and sealed with Teflon tape or Parafilm, some were left open to the atmosphere, and some were covered with various numbers of holes punched in the cuvette cap. Regardless of the drying conditions, all of the gels cracked within 24 h.

Ethylene glycol, $HOCH_2CH_2OH$, (50 µL-300 µL) and cetyltrimethylammonium bromide (CTAB, 0.01 g-0.10 g) were later added to

this recipe. The former was added in an attempt to decrease the rate of drying, and the latter was used in hopes to prevent gel cracking. In spite of trying several different ratios of starting materials as well as different drying conditions, all of the *gel series 2-B* cracked within 24 h. The stress of the rigid rectangular container used as the mold for these gels may have contributed to the severe gel cracking.

2.2.1.c Preparation of Monoliths in Glass Vials (*Gel Series 2-C*)

In an attempt to decrease drying stress likely caused by the rigid cuvette mold, gels were prepared in 7 dram cylindrical glass vials. TMSen (100 µL-800 µL, 0.458 mmol-3.67 mmol), TMOS (455 µL, 3.08 mmol), MeOH (545 µL, 13.45 mmol) and CTAB (0.032 g, 0.088 mmol) were combined in a glass vial. The addition of 500 µL of H_2O caused extremely fast gelation and the release of heat from the starting mixture. Gels were initially colorless, and many of them cracked almost instantly into large pieces. The *gel series 2-C* did not crack into small, dust-like particles as other gel series had, even after 24 h. The pieces of gel were however too small to use in Cu^{2+} ion uptake experiments, and the procedure thus had to be modified to produce larger pieces of gel.

2.2.1.d Preparation of Monoliths in Petri Dishes (*Gel Series 2-D*)

In a glass vial, TMOS (6.00 mL, 40.7 mmol), CTAB (0.0387 g, 0.106 mmol), MeOH (3.00 mL, 74.06 mmol), and 1.80×10^{-4} M NaOH (1.21 mL,

0.218 μmol) were combined with stirring. In a separate vial, TMSen (0.115 mL-1.844 mL, 0.527 mmol-8.45 mol) was mixed with MeOH (4.26 mL, 105 mmol). Solutions from the two vials were combined and immediately transferred to a 100 mm disposable Petri dish and covered with Parafilm. Gels formed within 5 s, and within 6 h the gels cracked into large pieces. These pieces were transferred to beakers and covered with water; approximately six usable pieces were obtained from each Petri dish.

Although these gels were extremely fragile, they were used in an initial kinetics study to investigate their spectroscopic behavior in Cu^{2+} solution. A gel holder, patterned after an infrared salt plate holder, was constructed of plastic materials. Both the gel and sample holder were submerged into 500 mL of $CuCl_2$ solution (12.5-200 mM) for 1 min. The gel and holder were then quickly removed from the solution and placed in the light path of a Hewlett Packard 8452A diode array spectrometer where the absorbance at 620 nm was recorded. The gel and holder were then returned to the Cu^{2+} solution for 1 min, and this procedure was repeated for a total of 11 min. Plots of absorbance at 620 nm vs. time were somewhat linear ($R^2 > 0.90$), and the slopes of these lines increased with increasing $[Cu^{2+}]$, suggesting a relationship between the absorbance spectra of complexes formed within the gel and the cupric ion concentration in solution.

Although these studies gave promising results, the monoliths in *gel series 2-D* prepared by this method were extremely delicate. Many of the gels used in these studies were fractured or broken when they were

removed from the Petri dish or placed in the gel holder. Also, the procedure for data acquisition was very tedious and could not be precisely reproduced even within a single experiment. In order to develop a system that could be used in environmental applications, more robust monoliths and a simple, more reliable method for data acquisition were essential.

2.2.2 The Ligand-Grafting Technique

Physically robust sol-gel monoliths of good optical quality could easily be prepared using only inorganic precursors; the addition of the organic amine ligand to the starting mixture was likely the cause of poor gel quality. Because the TMSen ligand contains the $-Si(OCH_3)_3$ functional group, this ligand is capable of covalent bonding during the sol-gel process. A new approach was thus developed in which a purely inorganic sol-gel monolith was first prepared and the TMSen ligand was then added at a later stage after gelation was complete. Several different variables in the gel preparation method were investigated and optimized, including the ratios of starting materials, effects of catalysts and additives, and the conditions during the grafting, aging, and drying steps. The gels described here were strong and colorless and could be used in Cu^{2+} uptake studies.

2.2.2.a Preparation of a Blank Sol-Gel Monolith (*Gel 2-E*)

MeOH (225 µL, 5.55 mmol), TMOS (225 µL, 1.53 mmol), and ethylene glycol (115 µL, 2.06 mmol) were mixed with stirring in a 1 dram

glass vial. The stir bar was removed and 50 mM NaOH (135 µL, 6.75 µmol) was added to this mixture. Gelation was complete within approximately 3 min. The freshly prepared gel was covered with MeOH and the vial was capped and allowed to stand overnight. The MeOH was removed, and the gel was allowed to shrink to approximately 80% of its initial diameter in air for approximately 8 h. The 1-1.5 cm diameter disk was again covered with MeOH and allowed to stand overnight. The MeOH solution was decanted off and replaced stepwise with 75% MeOH, 50% MeOH, 25% MeOH, and finally pure water to avoid gel cracking. The water above the gel was changed several times before use to give blank *gel 2-E*. *Gel 2-E* was used as the reference in all spectroscopic experiments.

2.2.2.b Preparation of a Ligand-Grafted Sol-Gel Monolith (*Gel 2-F*)

MeOH (225 µL, 5.55 mmol), TMOS (225 µL, 1.53 mmol), and ethylene glycol (115 µL, 2.06 mmol) were combined, with stirring, in a glass vial (1 dram). The stir bar was removed, and after 50 mM NaOH (135 µL, 6.75 µmol) was added to the mixture, a gel started to form within approximately 3 min. The freshly prepared gel was covered with MeOH and allowed to stand overnight. The MeOH was removed, and the gel was allowed to shrink to approximately 80% of its initial diameter in air. The 1-1.5 cm diameter disk was again covered with MeOH and allowed to stand overnight. A 37.5 µL portion of TMSen (0.172 mmol) was added to the MeOH over the gel, and the vial was capped and placed on a mechanical

shaker overnight. Deionized water (1 mL) was added to the solution above the gel, and the vial was again placed on the mechanical shaker overnight. The solution above the gel was decanted off and replaced with 100% MeOH and allowed to stand overnight. To ensure that the TMSen ligand had grafted completely to the sol-gel monolith, approximately 1.5 mL of 50 mM $CuCl_2$ solution was added to the supernatant solution. This solution did not change to the intense blue color of the Cu^{2+}:ligand complex, indicating that the grafting procedure was successful and the ligand was covalently bound to the sol-gel monolith. The MeOH solution was decanted off and replaced stepwise with 75% MeOH, 50% MeOH, 25% MeOH, and finally pure water to avoid gel cracking. The water above the gel was changed several times prior to use to give *gel 2-F*. The preparation of *gel 2-F* is shown schematically in **Figure 2.1**.

2.2.3 Characterization Studies

Characterization studies were performed in an attempt to describe the physical characteristics of the sol-gel monoliths. Metal ion transport through the gel interior depends partially on the physical properties of the solid material, such as the pore size, pore volume, and surface area. Brunauer Emmett Teller (BET) gas adsorption studies were performed by standard methods to give a better understanding of the physical properties of the ligand-grafted *gel 2-F*. Scanning electron microscopy (SEM) was used to visualize the surface of a typical *gel 2-F* and to obtain the

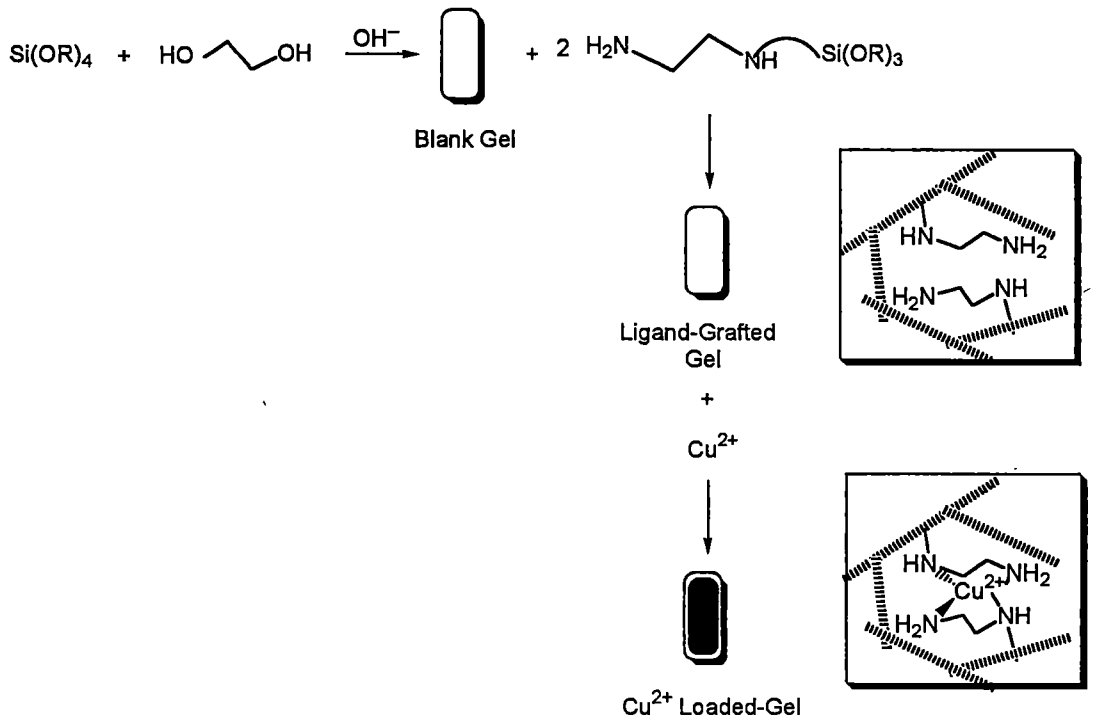

Figure 2.1. Schematic of the preparation of the diamine ligand-grafted *gel 2-F*.

morphology of the surface. Images were collected at 150,000X and 180,000X magnification. Sol-gel samples were mounted on carbon tape and sputtered with gold to increase conductivity and avoid the build-up of negative charge before SEM image collection.

2.2.4 Spectroscopic Measurements

The tungsten halogen source lamp of the spectrometer was allowed to warm for 30 min before each set of experiments. The blank *gel 2-E* was mounted into the compartment of the gel holder/flow cell. A $CuCl_2$ solution (500 mL) was then pumped through the system at a flow rate of approximately 60 mL/min. After 2 min, a reference spectrum was recorded. The light path from the source was blocked and a dark spectrum was recorded. The blank *gel 2-E* was removed, and both the gel holder and the tubing were dried thoroughly. Both the reference spectrum and the dark spectrum were subtracted from each subsequent spectrum. A ligand-grafted *gel 2-F* was then placed into the gel holder. Upon the initiation of the pump, a complete spectrum over the range of 400-850 nm was recorded every 20 sec for 15 min. From the collected data, λ_{max}, as well as any background interference could be determined. The data could then be analyzed to produce a plot of corrected absorbance *A* (at λ_{max}) vs. time. This procedure was then repeated at each Cu^{2+} concentration used in the study.

2.2.5 Cu^{2+} Removal

Cu^{2+} ions were removed from *gel 2-F* by placing the gel on a mechanical shaker in approximately 3 mL of 1.0 M HCl. This HCl solution was changed several times until a colorless gel was observed. The gel was then washed several times with distilled water. In an attempt to neutralize the gel, it was placed in 3 mL of either 0.10 M NaOH (pH = 13) or 0.667 mM $NaHCO_3$ (pH = 8). The gel was then rinsed several times with distilled water before use.

Attempts were also made to remove Cu^{2+} ions from *gel 2-F* by placing the gel on a mechanical shaker in 3 mL of 0.10 M EDTA or in 3 mL of anhydrous ethylenediamine solution. However, the gel remained an intense blue color while the solution above the gel remained colorless, indicating that the Cu^{2+} ions were not removed from the gel.

2.2.6 Reproducibility Study

The spectroscopic behavior of several *gels 2-F* (neutralized with either NaOH or $NaHCO_3$) was measured through two cycles of Cu^{2+} uptake and removal. These experiments were carried out as described previously in 75.03 mM [Cu^{2+}].

2.3 Results and Discussion

Several methods were used in an attempt to prepare crack-free, ligand-grafted sol-gel monoliths. Once the preparation of these monoliths

was successfully developed and optimized, the ligand-grafted monoliths were found to bind Cu^{2+} ions to form an intense blue complex that could be measured by spectrophotometry. The rate of formation of the blue complex could be correlated to the [Cu^{2+}] in solution. This method was used in optical fiber metal fluorosensors,[42] and was recently reviewed.[41a] Sol-gel monoliths prepared in different batches by the same method gave similar results, indicating that the preparation method developed here was highly reproducible. Cu^{2+} ions could be removed from the gels by washing with HCl, but neutralization with base was not achieved. The physical integrity of the gel was found compromised when it was placed in solutions of high pH. Spectroscopic results using these gels were not reproducible from the 1st to 2nd cycle. The sol-gel monoliths grafted with amine ligands described here could be used as an irreversible, one-time use, Cu^{2+} ion probe.

2.3.1 Preparation of a Ligand-Grafted Sol-Gel Monolith (Gel 2-F)

The sol-gel process involves the hydrolysis and polycondensation of alkoxide precursors such as $Si(OR)_4$ at room temperature to yield inorganic glasses. Sol-gels are particularly well suited for substrates in optical analysis partly because they are transparent in the visible region.[52] The porosity of the final glass product is easily varied, allowing the incorporation of chelating molecules into the glass matrix and supporting the fast transport of small molecules throughout the gel interior. There are two main methods for the incorporation of organic molecules into a sol-gel glass: doping and

immobilization (or grafting).[25,26,53] Chemical doping is highly versatile because organic molecules are simply encapsulated within the matrix of the gel by engineering the gel porosity. Recent studies within our research group of this approach have led to SiO_2 sol-gel as well as SiO_2-ZrO_2-polymer blend thin films doped with dyes as optical sensors for highly acidic ($[H^+]$ = 1-11 M) and basic ($[OH^-]$ = 1-10 M) solutions, respectively.[54-57] However, since the molecules used to register the presence of these targets are not chemically bound to the gel interior, they often leach out over time, and the sensor must be re-calibrated, increasing the time and cost for analysis. In the immobilization technique, a functional group of the reagent molecule is chemically bound to the sol-gel matrix, and therefore reagent leaching is not expected in chemically grafted gels.[25,26,53]

During the drying period in the formation of sol-gel glasses, a pressure gradient in the liquid phase of the gel is produced, leading to different rates of shrinkage within the network. When the exterior of the gel shrinks at a higher rate than the interior of the gel, tensile stresses arise that lead to fracture of the network. Cracking of the glass often occurs because the stress in the gel network exceeds its strength. In purely inorganic systems, this cracking may be prevented by increasing the aging time so the gel develops adequate strength to reduce cracking during the drying stage, increasing the pore size to decrease capillary pressure, or by the addition of chemical additives which may decrease capillary stress or allow for faster drying.[21] However, crack prevention is often much more difficult in

inorganic-organic hybrid materials, because the network is not composed exclusively of –Si-O-Si- bonds. Several different gel preparation methods were tested before the current approach was developed to give ligand-grafted gels with little or no cracking. In this approach, the formation of a purely inorganic sol-gel monolith, followed by the addition of the organic ligand after gelation is complete, seems to be the most important factor in crack prevention. The use of ethylene glycol, which may act as a spacer molecule to decrease the pressure gradient, leads to uniform mesopores throughout the bulk of the gel. In addition, adequate aging and slow drying at ambient temperature and pressure also appear to aid in crack prevention.

2.3.2 Characterization by BET and SEM

BET gas adsorption experiments indicate that the ligand-grafted *gel 2-F* is a mesoporous material with an average pore diameter of 64 Å. **Figure 2.2** shows the 10-point BET plot, which is linear over the actual relative pressure range of 0.04-0.36. A plot of pore volume as a function of pore diameter, shown in **Figure 2.3**, indicates that *gel 2-F* has a narrow pore size distribution consistent throughout the bulk of the material. The peak of this plot near 60 Å represents the size of pores that contribute most to the pore volume. **Figure 2.4** shows the N_2 adsorption isotherm plot, which again indicates that *gel 2-F* is quite porous. The adsorption isotherm shows a well-defined Z-shaped hysteresis loop in which the adsorption path lies below the desorption path. This hysteresis loop is common in mesoporous

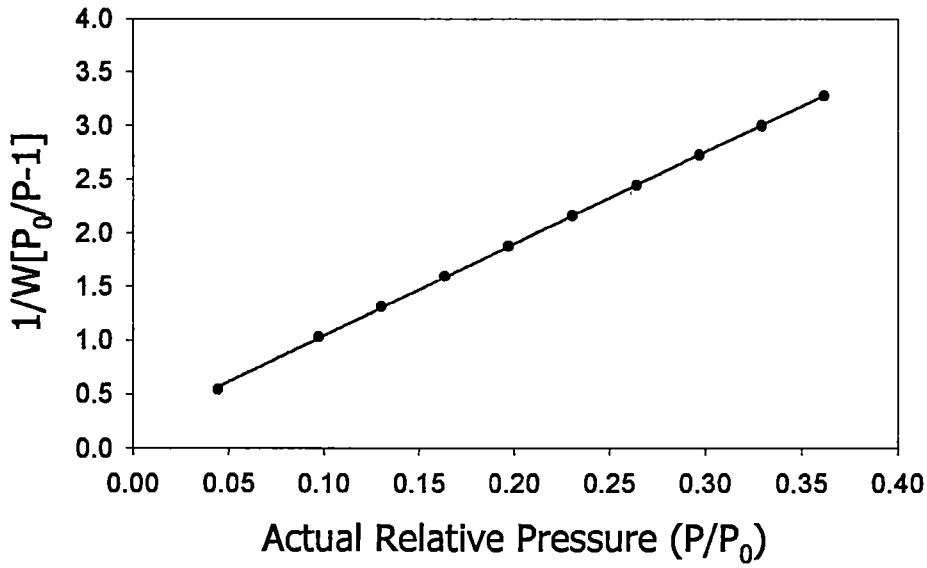

Figure 2.2. 10 point BET plot for diamine ligand-grafted *gel 2-F*.

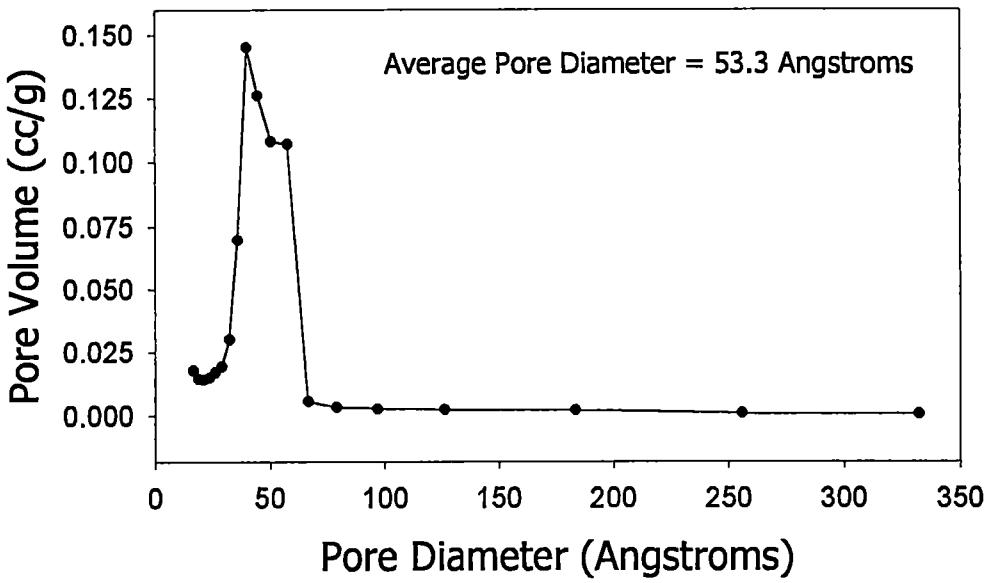

Figure 2.3. BET pore size distribution for diamine ligand-grafted *gel 2-F*.

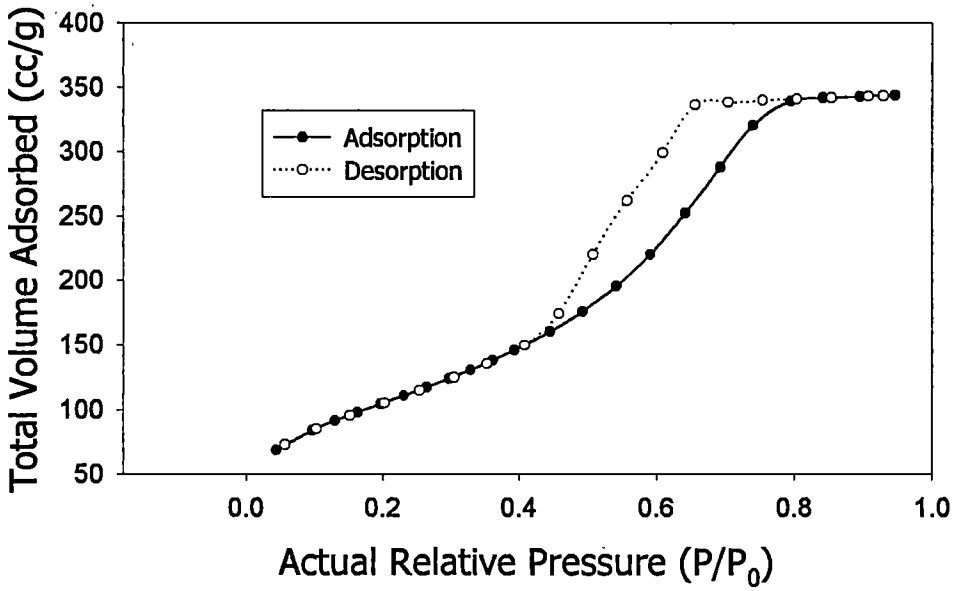

Figure 2.4. N_2 gas adsorption/desorption isotherms for diamine ligand-grafted *gel 2-F*.

materials including inorganic oxides and glasses.[58] The specific surface area of *gel 2-F* was 398 m^2/g, and the total pore volume was 0.531 cc/g of gel.

SEM images of *gel 2-F*, taken at 150,000X and 180,000X magnification, are shown in **Figure 2.5**. These images show that the sol-gel material is amorphous and that the surface is not smooth. The network of spherical particles packed together is representative of a base-catalyzed process in which colloidal silica clusters are initially formed and then linked through gelation.[24] Although the pores are quite large in base-catalyzed gels, these pores are too small to observe using SEM imaging.

2.3.3 Cu^{2+} Uptake and Determination

The visible absorbance spectra of a typical TMSen-grafted *gel 2-F* in 75.03 mM Cu^{2+} over a period of 2-12 min is shown in **Figure 2.6**. The Cu^{2+}:amine complex within the gel showed a broad absorbance band with a peak at 617 nm. Leyden and co-workers studied in detail the complexation of copper (II) with the ethylenediamine analog TMSen immobilized on silica gel.[59] They found consecutive formation of both the mono and the bis Cu^{2+}:TMSen complexes on the surface of the silica gel with increasing $[Cu^{2+}]$. Visible spectra in their work showed that both complexes exhibited broad absorption bands with maxima at 658 nm for the mono $Cu[TMSen]^{2+}$ complex and at 556 nm for the bis $Cu[TMSen]_2^{2+}$ complex. They also discovered that at very low $[Cu^{2+}]$, formation of the bis complex was favored

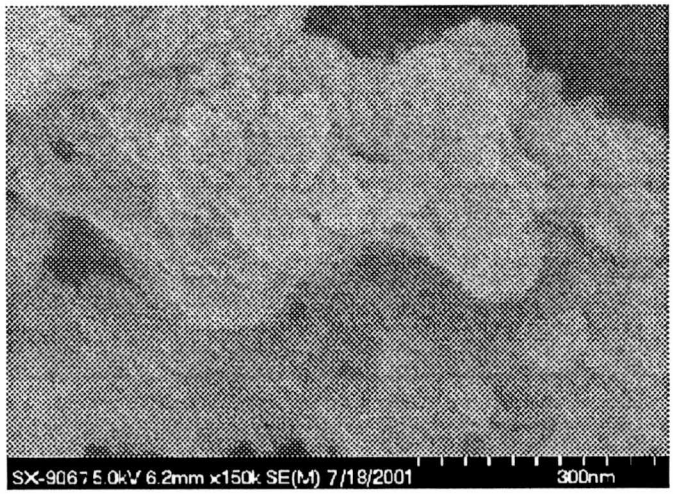

(a)

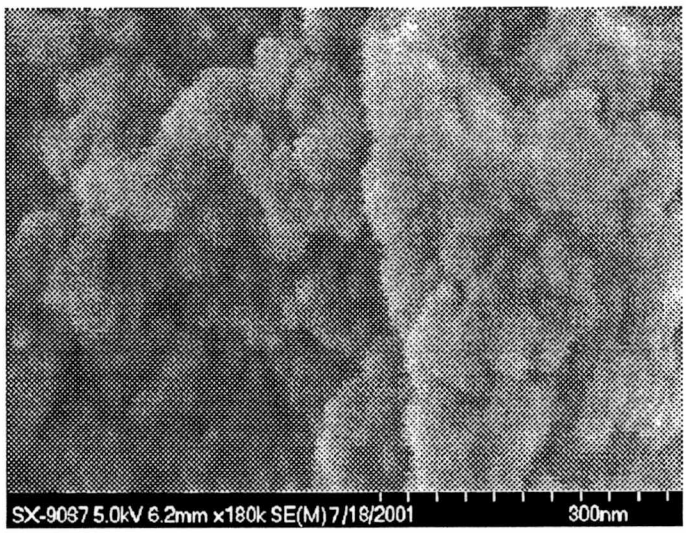

(b)

Figure 2.5. SEM images of diamine ligand-grafted *gel 2-F* at (a) 150,000X and (b) 180,000X magnification.

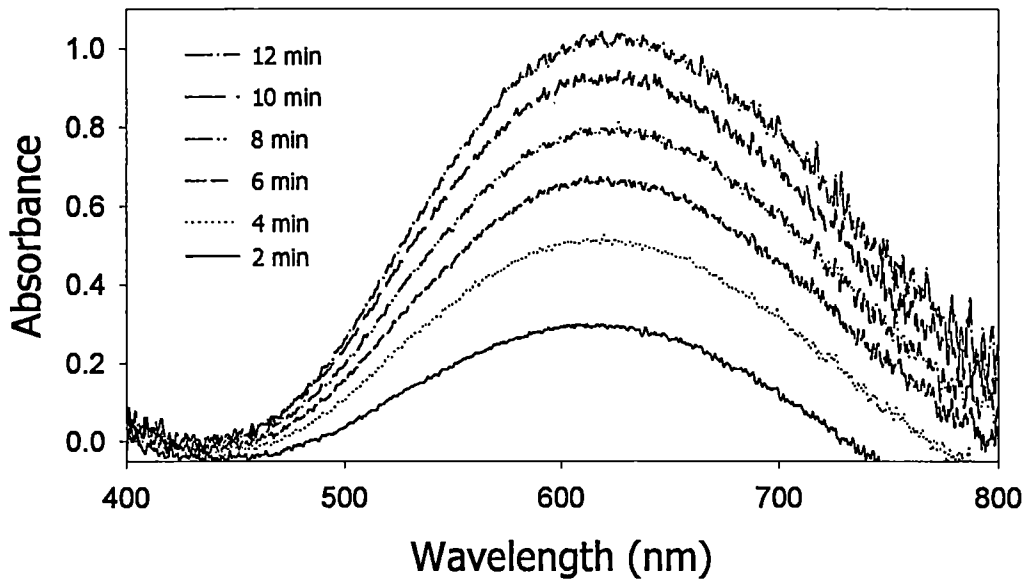

Figure 2.6. Absorbance spectra of a typical diamine ligand-grafted *gel 2-F* in 75.03 mM Cu^{2+} from 2-12 min.

because of its greater stability, but with increasing [Cu^{2+}], the mono complex made an increasing contribution to the absorbance spectrum. Our studies showed that in solution, λ_{max} = 635 nm for the mono complex, while the bis complex showed a peak at 558 nm. These spectra are shown in **Figure 2.7**. The relatively broad peak at 617 nm of *gel 2-F* in Cu^{2+} solution is consistent with the presence of a mixture of both the mono and the bis Cu^{2+}:TMSen complexes within the gel. It is important to note that λ_{max} for the complex within the gel did not change over the course of the experiment. Although there have been reports of the initial formation of the bis complex, followed by an increasing contribution from the mono complex,[59] the phenomenon was not observed in these studies as indicated by no observed peak shift with increasing Cu^{2+} saturation.

Figure 2.8 shows plots of absorbance (*A*) at 617 nm vs. time (*t*) for several typical diamine grafted *gels 2-F* in various [Cu^{2+}]. The baseline absorbance of these plots has been offset for clarity. These plots are fairly linear ($R^2 > 0.98$) over a period of 10 min, and they clearly show a relationship between the absorbance of the Cu^{2+}:TMSen complex within the gel at 617 nm and the concentration of copper (II) ion in solution. As the [Cu^{2+}] increases, the rate of Cu^{2+} diffusion into the gel increases, and the rate of formation of the blue Cu^{2+}:TMSen complex also increases. The slopes of these lines can then be plotted against the concentration of Cu^{2+} to obtain a calibration curve (**Figure 2.9**). Each point on the calibration curve

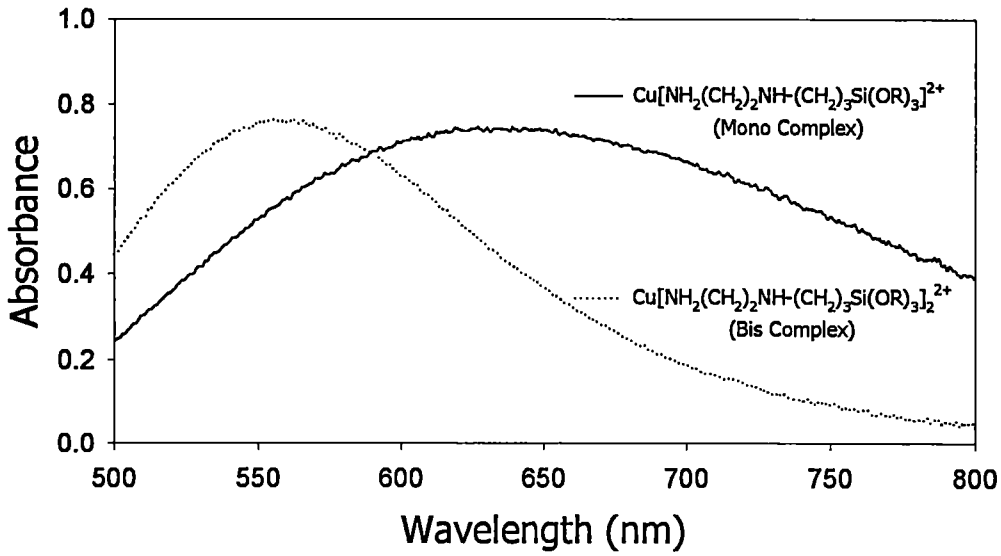

Figure 2.7. Absorbance spectra of $Cu[TMSen]_n^{2+}$ complexes.

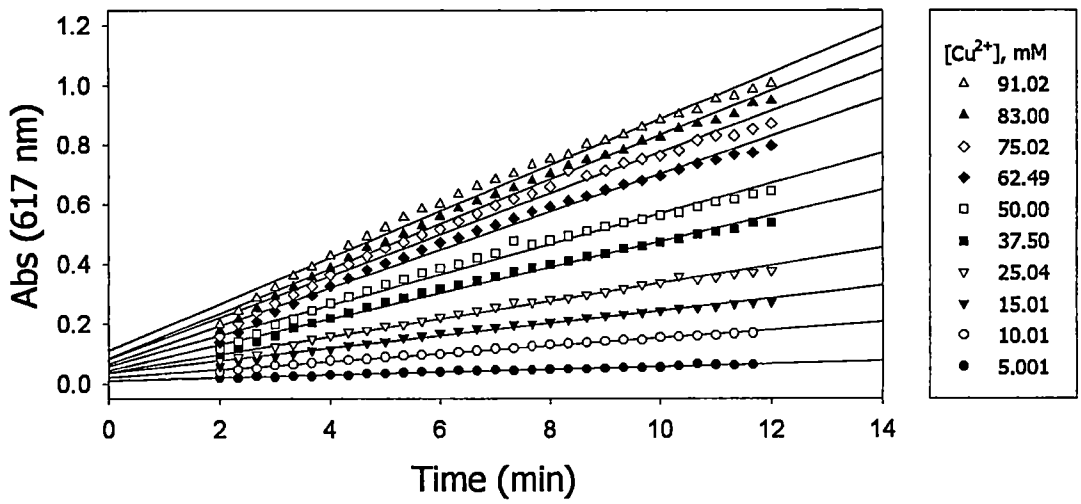

Figure 2.8. Absorbance vs. time plots of diamine ligand-grafted *gels 2-F* in various [Cu^{2+}] from 2-12 min. Baseline has been offset for clarity.

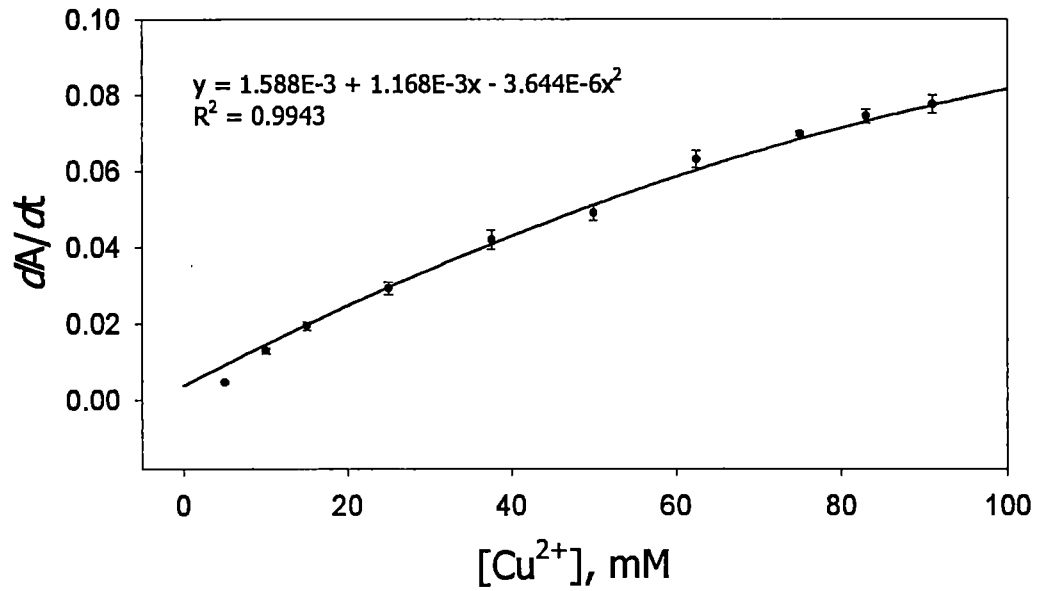

Figure 2.9. Correlation between slopes *dA/dt* from 2-12 min and $[Cu^{2+}]$ for diamine ligand-grafted *gels 2-F.*

is an average taken from at least five different gels. The curve is fairly linear in the concentration range of 5.00-75.02 mM Cu^{2+} (R^2 = 0.9866), but is better described by a polynomial curve fit. From 5.00-91.02 mM Cu^{2+}, the plot of dA/dt vs. $[Cu^{2+}]$ fits the equation, $y = ax^2 + bx + c$, with R^2 = 0.9973. Although the slope (dA/dt) and $[Cu^{2+}]$ are not directly proportional, the 2nd order polynomial curve fit still provides a simple mathematical relationship between these two variables. The limit of detection using this method was 5.00 mM Cu^{2+}; below this concentration, the absorbance signal of the gel could not be differentiated from background noise, and the slope of the absorbance vs. time plot did not change during the 10 min period studied. At Cu^{2+} concentrations above 91.02 mM, the gels quickly become saturated with Cu^{2+} ions and the calibration curve is no longer valid. Although there are more Cu^{2+} ions in solution at high concentrations, these ions are possibly unable to diffuse into the gel interior at a rate faster than observed in 91.02 mM Cu^{2+} solution due to the relatively small pore diameter of the gels.

The results for the diamine grafted sol-gel monoliths prepared in the same batch as well as between batches were similar, indicating that the gel preparation method was highly reproducible. Within a single Cu^{2+} uptake-removal cycle, the difference in dA/dt for gels prepared at the same time (within the same batch) ranges from 0.52-5.6%. The data shown in the calibration curve is for a single Cu^{2+} uptake-removal cycle of five separate batches of gels, all prepared by the same method but at different times

within a six month period. Gels from separate batches were stored in water for different amounts of time prior to use, and yet the results from each of these five batches are similar.

2.3.4 Cu^{2+} Removal and Sensor Regeneration

In order to develop an optical ion sensor for multi-cycle use, Cu^{2+} ions must be removed completely from the gel interior between cycles. Cu^{2+} ions could be removed from *gels 2-F* using 1.0 M HCl, but complete neutralization of these gels with base for use in subsequent Cu^{2+} uptake-removal cycles was not possible. When gel neutralization using 0.10 M NaOH (pH = 13) was attempted, it is possible that the physical characteristics of the gel were compromised, considering that the monolith was comprised mostly of SiO_2, which is known to decompose at pH 12. Neutralization with $NaHCO_3$ was not possible; regardless of the number of times the basic solution above the gel was changed, the pH of the gel remained at approximately pH 4-5. When the absorbance of these gels at 617 nm vs. time was plotted, the error between several 2nd cycle gels ranged from 4.90-11.78%. In addition, the 2nd cycle *dA/dt* data acquired from gels washed with acid and then neutralized with base showed poor agreement with data from freshly prepared 1st cycle gels. Since it was impossible to fully neutralize the *gels 2-F* without physical degradation, multi-cycle [Cu^{2+}] determinations could not be performed, and the gels could

not be used as a reversible Cu^{2+} sensor, but rather a single-use only Cu^{2+} probe.

2.3.5 Decreasing Analysis Time

Real-time data is key for on-line chemical analysis. A long response time arising from slow kinetics can limit the application of sensors and probes. The probes described here require an analysis time of approximately 12 min, but it is possible to decrease this analysis time if a higher associated error is permissible. Absorbance vs. time plots for *gels 2-F* in various $[Cu^{2+}]$ are linear ($R^2 > 0.98$) from 2-4 min, as shown in **Figure 2.10**, and the slopes of these lines can be plotted against $[Cu^{2+}]$ to obtain a calibration curve (**Figure 2.11**) as described previously in Section 2.3.3. The error in this case is 4.78-13.02%, which may not be acceptable in some analytical situations. However, if the probe is to be used only for initial $[Cu^{2+}]$ measurements, where only a rough concentration estimate in a short period of time is necessary, this method of analysis may be useful.

2.4 Conclusions

Many of our attempts in the preparation of sol-gel monoliths grafted with amine ligands for the determination of $[Cu^{2+}]$ have been described. The challenges associated with the sol-gel processing of organic/inorganic hybrid materials were overcome to produce mechanically stable, optically transparent sol-gel discs containing functionalized amine ligands. These

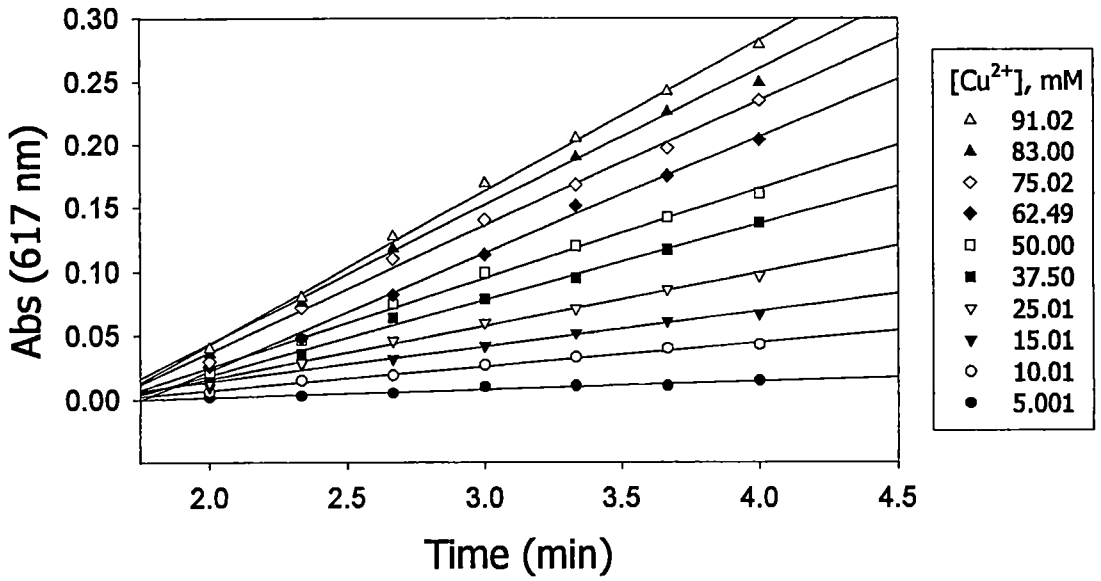

Figure 2.10. Absorbance vs. time plots of diamine ligand-grafted *gels 2-F* in various [Cu^{2+}] from 2-4 min. Baseline has been offset for clarity.

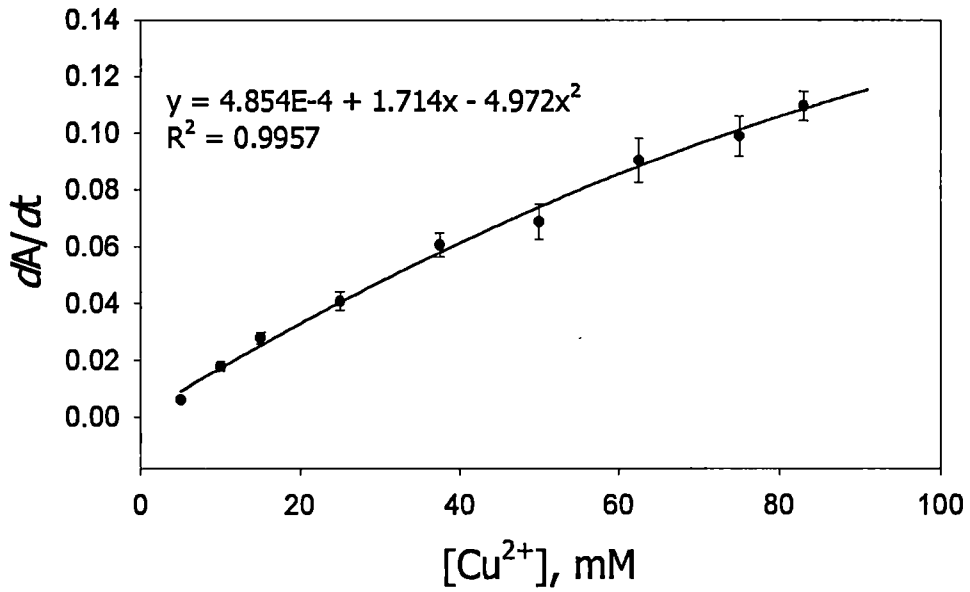

Figure 2.11. Correlation between slopes *dA/dt* from 2-4 min and $[Cu^{2+}]$ for diamine ligand-grafted *gels 2-F*.

discs could be used for the relatively quick determination of Cu^{2+} in the concentration range of 5.00-91.02 mM with reasonable experimental error. However, because of the strong binding between the ligand and the metal ions, these discs could not be regenerated and used in subsequent Cu^{2+} uptake/removal cycles. These sol-gel probes were therefore for single use only. These discs could easily be prepared in bulk from off-the-shelf chemicals, and results from sol-gel discs prepared by the same method at different times were reproducible.

CHAPTER THREE

IMPRINTED, MONOAMINE LIGAND-GRAFTED SOL-GEL MONOLITHS FOR MULTICYCLE COPPER (II) DETERMINATION

3.1 Introduction

Heavy metal ions, including copper (II), are commonly used in a variety of industrial applications. Copper electroplating is employed in many industrial processes, including the manufacture of next-generation microelectronic devices in the semiconductor industry.[9,11,60] Copper plating onto silicon wafers in very low acid or neutral solutions was recently developed.[11] Many heavy metal ions are considered pollutants as well. Specifically, copper (II) is recognized by the U.S. Environmental Protection Agency (EPA) as a toxic pollutant and is RCRA (Resource Conservation and Recovery Act) regulated.[13,39,61] Industrial metal ion concentrations are most often determined by techniques such as titration, atomic absorption, or atomic emission spectrometry. These procedures usually involve sample collection and some further treatment, such as the addition of reagents or dilution, and thus they may not be conducted on-line. Such analyses are often labor-intensive, making them costly, time-consuming, and inconvenient.

Chemical sensing is of intense current interest.[15,16,62] The optical sensing of metal ions in particular has been actively studied recently. Optical sensors offer the advantages of simple calibration, baseline control, and the versatility to measure several different analytes at once. In addition, they may be miniaturized and incorporated into portable systems.[20] Several heavy metal ion probes, for single use only, have been reported in the literature.[41a,43,44,46,47,63] The sensing mechanism of these probes often relies on strong interaction between the analyte ions of interest and an indicator or ligand immobilized on a solid state support. The binding between the metal ions and the indicator is often so strong that the removal of the analyte metal ions is difficult, either because the kinetics of release of the metal ion is slow, or because harsh conditions must be applied to fully remove the metal ion. Thus, these probes are usually for single-use only. The difficulty of creating a reversible metal ion sensor was encountered in our work with the diamine-grafted gels, as discussed in Chapter 2. These gels worked well for Cu^{2+} determination, but could not be regenerated and therefore could only be used as a one-time Cu^{2+} probe. A fully reversible sensor for multicycle Cu^{2+} determination must be developed for potential industrial use in the future.

There are few regenerable optical sensors for multi-cycle, quantitative metal ion measurements.[41a,64-67] Perhaps the simplest of these sensors is a method designed to monitor [Cu^{2+}] in an electroplating bath that relies only on the intrinsic optical absorption by Cu^{2+} ions in solution at 820 nm.[64] This

sensor is capable of measuring [Cu^{2+}] ranging from 50-500 mM with relative standard deviations less than 1%. Because no indicating reagents are necessary, the sensor may be reused. This sensor does suffer from some drawbacks, in that both the pH and temperature must be carefully controlled to avoid interferences. Other heavy metal ions would also likely interfere because they may absorb in this spectral region as well. Furthermore, since the sensor is not removed from the bath, conventional blank measurements cannot be obtained, and a two-wavelength measurement must be employed to correct for sensor drift. Another popular method of optical metal ion sensing is based on fluorescence spectroscopy. In 1988, Bright and co-workers described the development of a novel fluorimetric fiber-optic sensor for the determination of several different heavy metal ions.[66] Rhodamine 6G, a fluorophore, was immobilized on a Nafion film and its fluorescence was quenched by metal ions such as Co^{2+}, Cr^{3+}, Fe^{3+}, Fe^{2+}, Cu^{2+}, and Ni^{2+}. The rate of quenching was dependent on both the identity of the quenching ion and its concentration. Quenching by Cu^{2+} was fast, and the limit of detection was 1.2 μM [Cu^{2+}]. However, this sensor was not selective to one particular heavy metal ion, and the reproducibility over multiple cycles and the error associated with several measurements were not discussed in detail. More recently, an optical Cu^{2+} sensor was reported that combined electrochemical preconcentration of copper, elution of luminol and CN^- from an anion-exchange column, and luminescence of luminol, CN^-, and stripped copper.[67] This sensor was capable of measuring very low [Cu^{2+}] (0.01-10

μg/L) and it could be reused over 200 times with only ~8% error. However, the process requires multi-steps, and the method uses KCN, which is extremely toxic.

Functionalized bulk sol-gel materials grafted with ligands have been used successfully for the removal of heavy metal ions such as copper (II) from various solutions.[48-51] However, the preparation of a strong, crack-free, ligand-grafted sol-gel monolith is usually difficult, limiting the optical ion sensing applications of these materials. Often, ligand-grafted sol-gel materials such as powders or small particles are used as metal ion sorbents or in chromatography applications. Ligand-grafted sol-gel monoliths of optical quality for sensor applications have not been reported, despite the fact that sol-gels are particularly well suited as substrates in optical analysis.

A simple, novel process from off-the-shelf chemicals to give strong, crack-free, monoamine-grafted sol-gel monolith sensors for multi-cycle Cu^{2+} measurement in flowing solutions is reported. A templating approach was employed to graft the Cu^{2+}:ligand complex into the gels. The molecular imprinting approach used was found to provide enhanced Cu^{2+} binding, which is normally observed in multi-dentate ligand-grafted gels. Subsequent Cu^{2+} removal from the monodentate amine ligand within the monolith was achieved by the addition of ethylenediaminetetraacetic acid (EDTA), making regeneration of the sensors possible.

3.2 Experimental Section

The chemicals used in this study, including $H_2N(CH_2)_3Si(OMe)_3$ (3-aminopropyltrimethoxysilane (monoamine ligand), Aldrich, 97%), $Si(OCH_3)_4$ (TMOS, Aldrich, 98%), CH_3OH (MeOH, Mallinckrodt, 99.9%), and HO-CH_2CH_2-OH (Fisher, Certified), were used as received. Ultra-pure deionized water was used in the preparation of all gels and aqueous $CuCl_2$ solutions. Distilled water was used in gel washing. UV-visible spectrophotometry was performed on an Ocean Optics S2000 miniature fiber optic spectrophotometer interfaced to a computer for data collection using Ocean Optics OOIBase32 operating software. A flow-cell was designed to hold gels steady in flowing solution while supporting two fiber optic cables that were isolated from the solution. Gels used in these experiments were prepared in bulk; the following procedures are for the preparation of a single gel. Amounts of reagents were increased stoichiometrically to give the desired number of gels. All of the sol-gel monoliths were stored in deionized water before use. $CuCl_2$ solutions ranging in concentration from 5.00-99.98 mM were prepared gravimetrically using ultra-pure deionized water as the solvent. To avoid precipitation of the buffer anion and the metal cation, these solutions were not buffered.

3.2.1 Preparation of a Blank Sol-Gel Monolith (Gel 3-A)

MeOH (225 µL, 5.55 mmol), TMOS (225 µL, 1.53 mmol), and ethylene glycol (115 µL, 2.06 mmol) were mixed with stirring in a glass vial

(1 dram). After removing the stir bar and adding 50 mM NaOH (135 µL, 6.75 µmol) to this mixture, a gel started to appear in approximately 3 min. The freshly prepared gel was covered with MeOH and allowed to stand overnight. The MeOH was removed, and the gel was allowed to shrink to approximately 80% of its initial diameter in air. The 1-1.5 cm diameter disk was again covered with MeOH and allowed to stand overnight. The MeOH solution was decanted off and replaced stepwise with 75% MeOH, 50% MeOH, 25% MeOH, and finally pure water to avoid gel cracking. The water above the gel was changed several times before use to give blank *gel 3-A*. *Gel 3-A* was used as reference.

3.2.2 Preparation of a Ligand-Grafted Sol-Gel Monolith (Gel 3-B)

MeOH (225 µL, 5.55 mmol), TMOS (225 µL, 1.53 mmol), and ethylene glycol (115 µL, 2.06 mmol) were combined, with stirring, in a glass vial (1 dram). The stir bar was removed, and after 50 mM NaOH (135 µL, 6.75 µmol) was added to the mixture, a gel started to form in approximately 3 min. The freshly prepared gel was covered with MeOH and allowed to stand overnight. The MeOH was removed, and the gel was allowed to shrink to approximately 80% of its initial diameter in air. The 1-1.5 cm diameter disk was again covered with MeOH and allowed to stand overnight. $H_2N(CH_2)_3Si(OMe)_3$ (30.0 µL, 0.172 mmol) was added to the MeOH over the gel and the vial was placed on a mechanical shaker overnight. Deionized water (1 mL) was added to the solution above the gel,

and the vial was again placed on the mechanical shaker overnight. The solution above the gel was decanted off and replaced with 100% MeOH and allowed to stand overnight. The MeOH solution was decanted off and replaced stepwise with 75% MeOH, 50% MeOH, 25% MeOH, and finally pure water to avoid gel cracking. The water above the gel was changed several times prior to use to give *gel 3-B*.

3.2.3 Preparation of an Imprinted, Ligand-Grafted Monolith (Gel 3-C)

MeOH (225 µL, 5.55 mmol), TMOS (225 µL, 1.53 mmol), and ethylene glycol (115 µL, 2.06 mmol) were combined, with stirring, in a glass vial (1 dram). The stir bar was removed, and after 50 mM NaOH (135 µL, 6.75 µmol) was added to the mixture, a gel started to form in approximately 3 min. The freshly prepared gel was covered with MeOH and allowed to stand overnight. The MeOH was removed and the gel was allowed to shrink to approximately 80% of its initial diameter in air. The 1-1.5 cm diameter disk was again covered with MeOH and allowed to stand overnight. $H_2N(CH_2)_3Si(OMe)_3$ (30.0 µL, 0.172 mmol) was added to $CuCl_2$ (6.79 mg, 0.0398 mmol) dissolved in 1485 µL of MeOH to give a blue solution of $Cu[H_2N(CH_2)_3Si(OMe)_3]_4^{2+}$. This solution was added to the previously prepared gel and placed on a mechanical shaker overnight. A blue gel with a colorless supernatant was observed within 18 h. The supernatant solution was decanted off and replaced stepwise with 75% MeOH, 50% MeOH, 25% MeOH, and finally pure water. To remove Cu^{2+}, approximately 3 mL of

0.100 M EDTA (disodium salt) was added to the gel, which was then placed on a mechanical shaker. This EDTA solution was changed several times. When the gel appeared colorless, the EDTA solution was replaced with water, and the gel was washed with water several times to give *gel 3-C*. A schematic of the gel preparation procedure is shown in **Figure 3.1**.

3.2.4 Characterization Studies

Experiments were designed to better understand the physical characteristics of the sol-gel sensors. As noted previously, the kinetics of metal ion uptake is strongly influenced by the physical properties of the sol-gel monoliths. Brunauer Emmitt Teller (BET) gas adsorption studies were performed by standard methods to determine the pore size, pore volume, and surface area of the imprinted, ligand-grafted *gel 3-C* from which Cu^{2+} ions had been removed. Scanning electron microscopy (SEM) was also used to visualize the surface of a typical *gel 3-C*. Images were collected at 45,000X and 130,000X magnification. Sol-gel samples were placed on carbon tape and sputtered with gold prior to SEM image collection.

3.2.5 Spectroscopic Measurements

The tungsten halogen source lamp of the spectrometer was allowed to warm for 30 min before each set of experiments. The blank *gel 3-A* was mounted into the compartment of the gel holder/flow cell. A $CuCl_2$ solution (500 mL) was then pumped through the system at a flow rate of

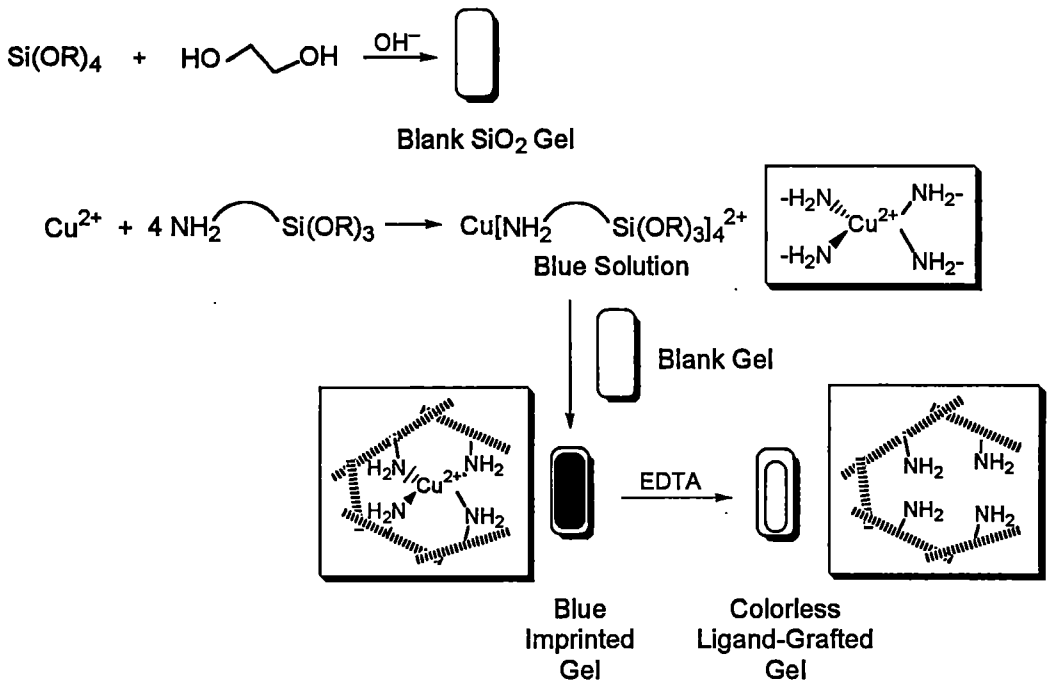

Figure 3.1. Schematic of the preparation of the imprinted, monoamine ligand-grafted *gel 3-C*.

approximately 60 mL/min. After 2 min, a reference spectrum was recorded. The light path from the source was blocked and a dark spectrum was recorded. The blank *gel 3-A* was removed, and both the gel holder and the tubing were dried thoroughly. Both the reference spectrum and the dark spectrum were subtracted from each subsequent spectrum. An imprinted, ligand-grafted *gel 3-C* was then placed into the gel holder. Upon the initiation of the pump, a complete spectrum over the range of 400-850 nm was recorded every 20 s for 15 min. From the collected data, λ_{max}, as well as any background interference could be determined. The data could then be analyzed to produce a plot of corrected absorbance A (at λ_{max}) vs time. This procedure was then repeated at each Cu^{2+} concentration used in the study.

3.2.6 Cu^{2+} Removal

Cu^{2+} ions were removed from *gel 3-C* by placing the gel on a mechanical shaker in approximately 3 mL of 0.100 M EDTA. This EDTA solution was changed several times until a colorless gel was observed. The gel was then washed several times with distilled water prior to further experiments.

3.2.7 Reproducibility Study

The spectroscopic behavior of four separate gels was measured through five cycles of Cu^{2+} uptake and removal. These experiments were carried out

as described previously in 75.03 mM [Cu^{2+}].

3.3 Results and Discussion

The ligand-grafted monoliths prepared in this study were found to bind Cu^{2+} ions to form a blue complex that could be measured by spectrophotometry. The rate of the formation of the complex was directly proportional to the [Cu^{2+}] in solution. This method was used in optical fiber metal fluorosensors,[42] and was recently reviewed.[41a] Sol-gel sensors prepared in different batches gave similar results, indicating that the preparation method was highly reproducible. These sol-gel sensors were regenerated with EDTA and results were reproducible for up to five cycles, showing the potential of these materials for use as true optical ion sensors.

3.3.1 Preparation of a Crack-Free, Imprinted, Ligand-Grafted Sol-Gel Monolith (Gel 3-C)

The sol-gel process refers to a series of reactions involving metal alkoxide precursors to prepare inorganic glasses. The properties of the final glass product can be varied by a number of factors, including the alkoxide precursor chosen, the pH of the solution, the types and concentrations of solvents, catalysts, and additives, and the conditions employed during aging and drying. The mild conditions used in the sol-gel process make possible the incorporation of a wide variety of organic molecules, including organic ligands that may be chemically grafted throughout the bulk of the

material.[21,23] Functionalized ligands of the form L-Si$(OR)_3$ can be anchored into the sol-gel matrix, and because the ligand, L-, is covalently bonded to both the external and internal surfaces of the porous material, ligand leaching is not a problem.

In molecular imprinting through the sol-gel process, a template molecule or ion associates with functionalized ligands to form a complex. Subsequent polymerization results in trapping the template molecule in the highly cross-linked sol-gel matrix. Removal of the imprinted molecule leaves a predetermined arrangement of ligands and a tailored binding site. These binding sites are the ideal size, shape, and chemical environment to rebind the imprinted molecule selectively.[68-74] The process of molecular imprinting in this approach of grafting ligands into the sol-gel matrix was essential. When amine ligands such as $H_2N(CH_2)_3Si\equiv$ are grafted through a non-imprinting process without a template, as shown in **Figure 3.2**, the four ligands are arranged randomly in the gels, and are not likely to be in positions to form $Cu[H_2N(CH_2)_3Si\equiv]_4^{2+}$ complexes. However, if the $Cu[H_2N(CH_2)_3Si\equiv]_4^{2+}$ complex is formed before the ligands are grafted to the sol-gel matrix, as in **Figure 3.3**, the removal of the metal ion produces a tailored cavity which, upon subsequent addition of the metal ion, is the ideal size and shape to rebind the metal ion within the predetermined

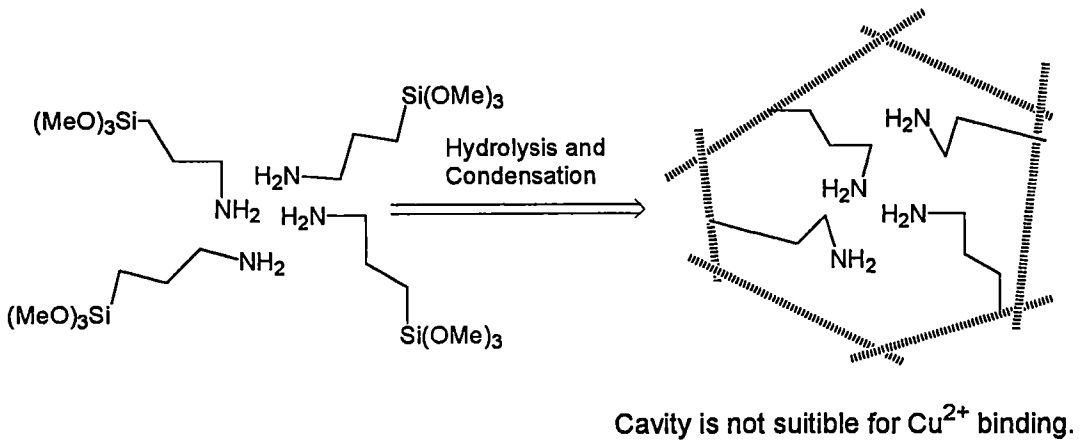

Figure 3.2. Conventional grafting (non-imprinting) procedure.

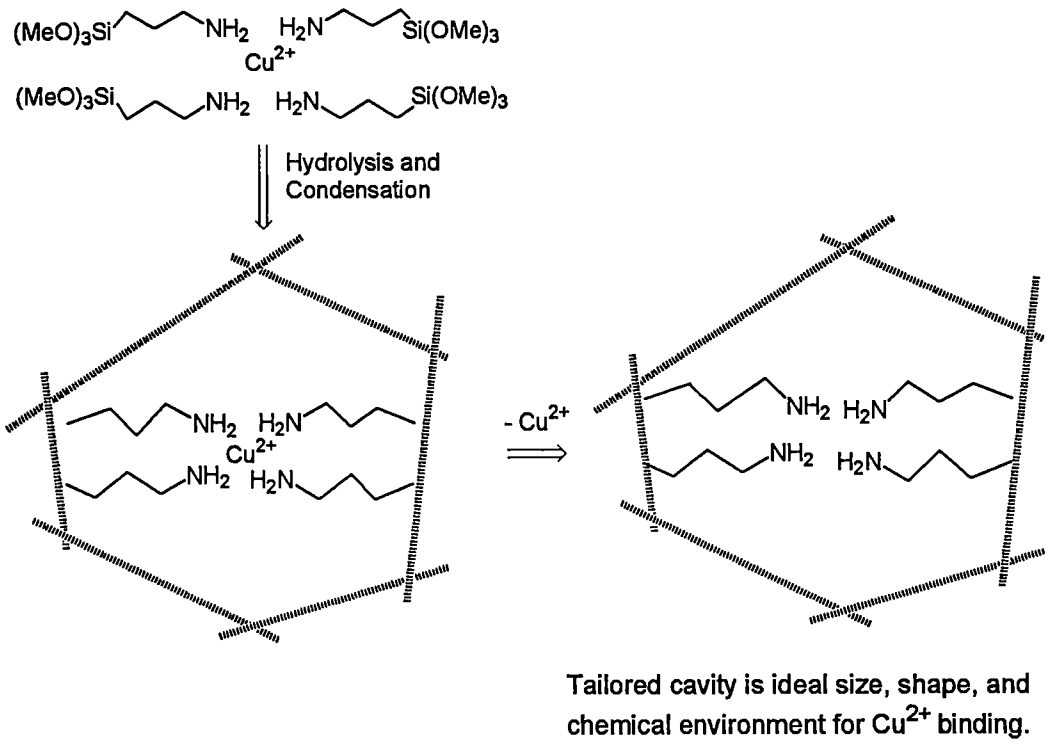

Figure 3.3. Imprint coating procedure.

arrangement of ligands. When the amine-grafted, non-imprinted *gel 3-B* was placed in Cu^{2+} solutions for spectroscopic measurement, a light blue $Cu(OH)_2$ solid precipitated within the structure of the gel. Further studies involving *gel 3-B* were discontinued because the formation of this precipitate could not be avoided. However, when the imprinted *gel 3-C* was placed in Cu^{2+} solutions, no precipitate was observed, and *gel 3-C* removed Cu^{2+} from the solutions to give a clear blue gel suitable for optical sensing.

3.3.2 Characterization by BET and SEM

BET gas adsorption studies indicate that *gel 3-C* is a mesoporous material with a specific surface area of 203 m^2/g, a total pore volume of 0.167 cc/g, and an average pore diameter of 33 Å. The 10-point BET plot of this gel is shown in **Figure 3.4**; this plot is linear over the actual relative pressure range of 0.04-0.36. **Figure 3.5** shows a plot of pore volume as a function of pore diameter and indicates that the distribution of pore sizes within *gel 3-C* is narrow and consistent throughout the bulk of the material. The peak of this plot near 33 Å represents the size of pores that contribute most to the pore volume. The N_2 adsorption isotherm plot is shown in **Figure 3.6**. The adsorption isotherm shows a well-defined Z-shaped hysteresis loop in which the adsorption path lies below the desorption path. This hysteresis loop also indicates mesoporosity.

SEM was used to study the surface morphologies of the imprinted, ligand-grafted *gel 3-C*. Two images were taken at different magnifications,

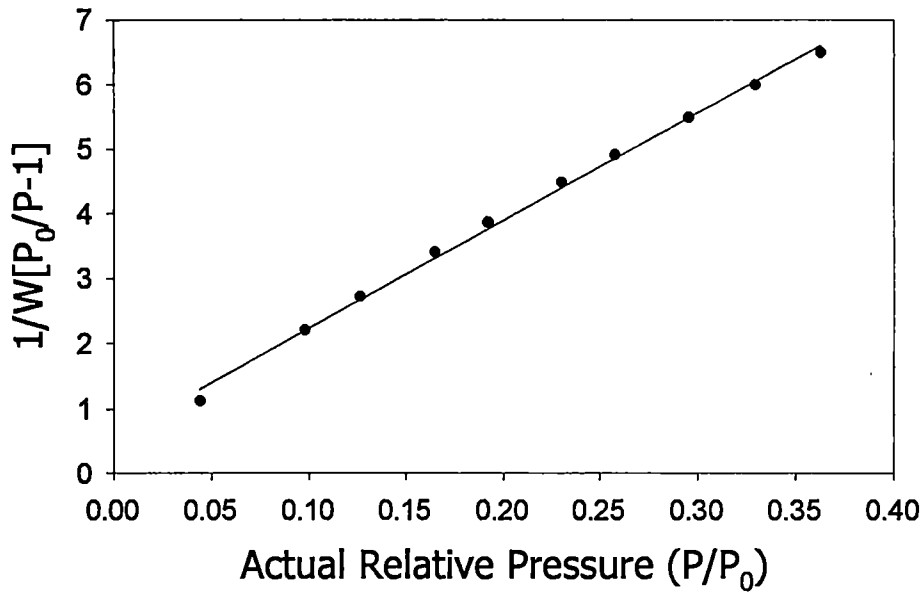

Figure 3.4. 10 point BET plot for imprinted, monoamine ligand-grafted *gel 3-C*.

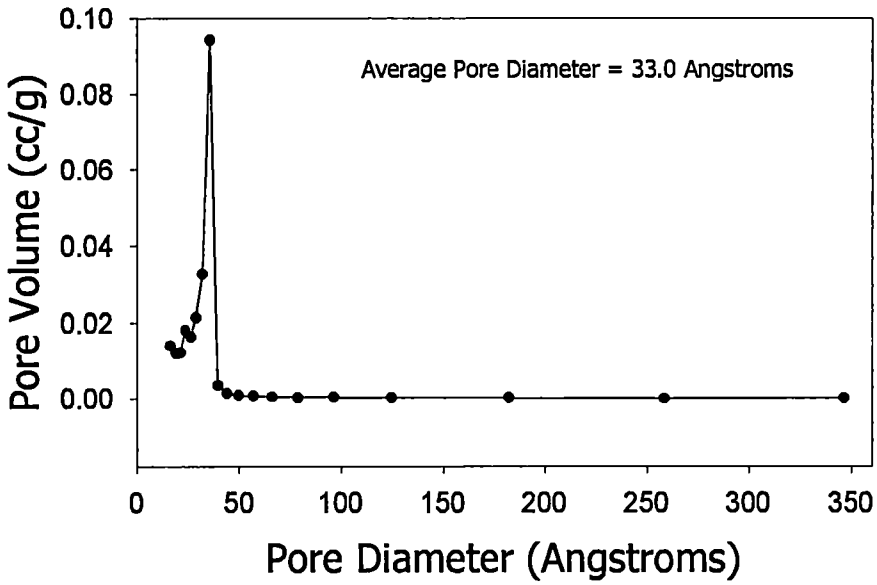

Figure 3.5. BET pore size distribution for imprinted, monoamine ligand-grafted *gel 3-C*.

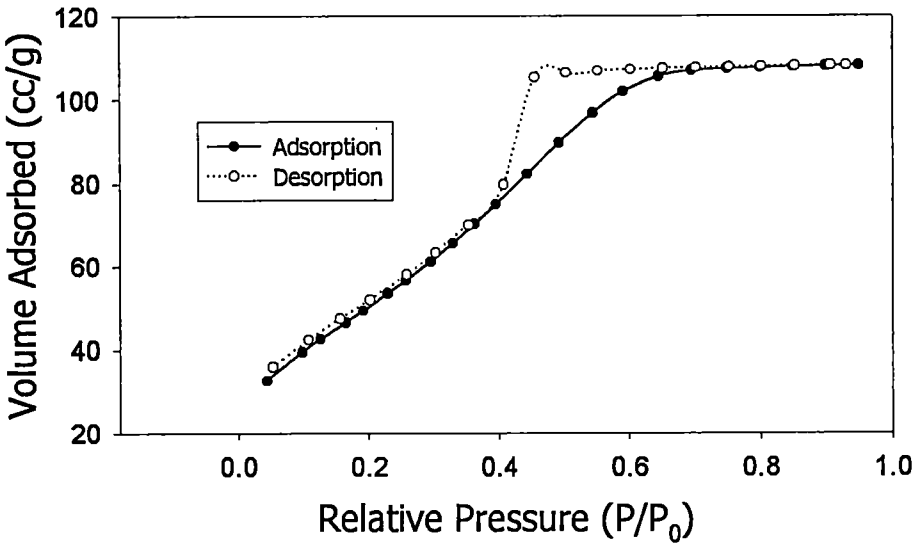

Figure 3.6. N_2 gas adsorption/desorption isotherms for imprinted, monoamine ligand-grafted *gel 3-C*.

and these images are shown in **Figure 3.7**. The image at 45,000X shows that the surface of the gel is irregular, and yet fairly smooth. Upon higher magnification (130,000X), large spherical clusters with an average diameter of approximately 500 nm, typical of base-catalyzed sol-gels, are observed.

3.3.3 Cu^{2+} Uptake and Sensing

The visible absorbance spectra of a typical monoamine grafted, imprinted *gel 3-C* in 75.03 mM Cu^{2+} over a period of 2-12 min is shown in **Figure 3.8**. The Cu^{2+}:amine complex within the gel showed a broad absorbance band with a peak at 730 nm. Klonkowski and coworkers have recently studied in detail the coordination environment of Cu(II)/$H_2N(CH_2)_3Si\equiv$ complexes grafted onto preformed silicate sol-gels.[75] The gels were characterized by IR, visible and electron spin resonance (ESR) spectroscopies. These studies suggested the presence of an elongated tetragonal-octahedral $Cu(H_2O)_5(H_2N(CH_2)_3Si\equiv)$ complex in the gels. Their gel preparation method was not identical to the method used in the current studies, but a xerogel analogous to our *gel 3-C* showed an absorbance maximum at approximately 650 nm. Our studies showed that in solution, λ_{max} = 700 nm for the $Cu[H_2N(CH_2)_3Si(OMe)_3]_4^{2+}$ molecular complex, while the Cu^{2+}:EDTA complex showed a peak at 740 nm, and $CuCl_2$ showed a very broad peak at 810 nm. These spectra are shown in **Figure 3.9**. To ensure that the peak observed at 730 nm was not from the

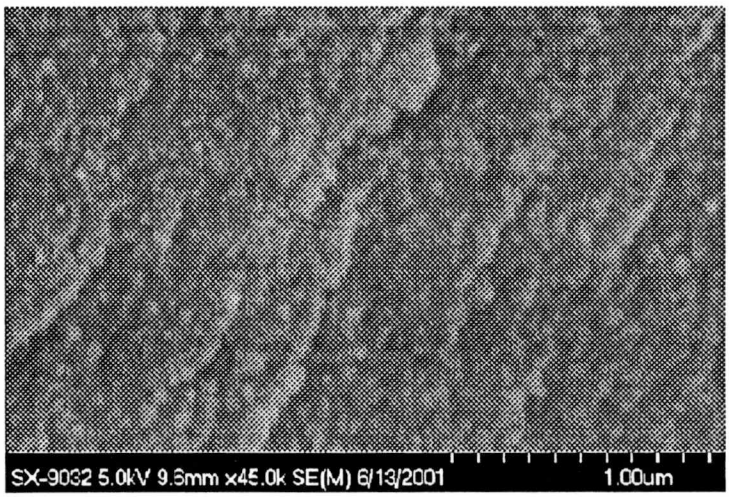

(a)

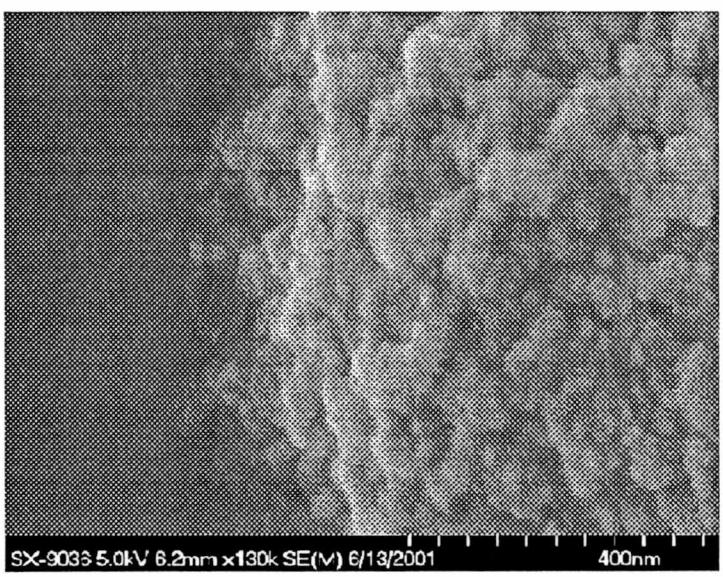

(b)

Figure 3.7. SEM images of imprinted, monoamine ligand-grafted *gel 3-C* at (a) 45,000X and (b) 130,000X magnification.

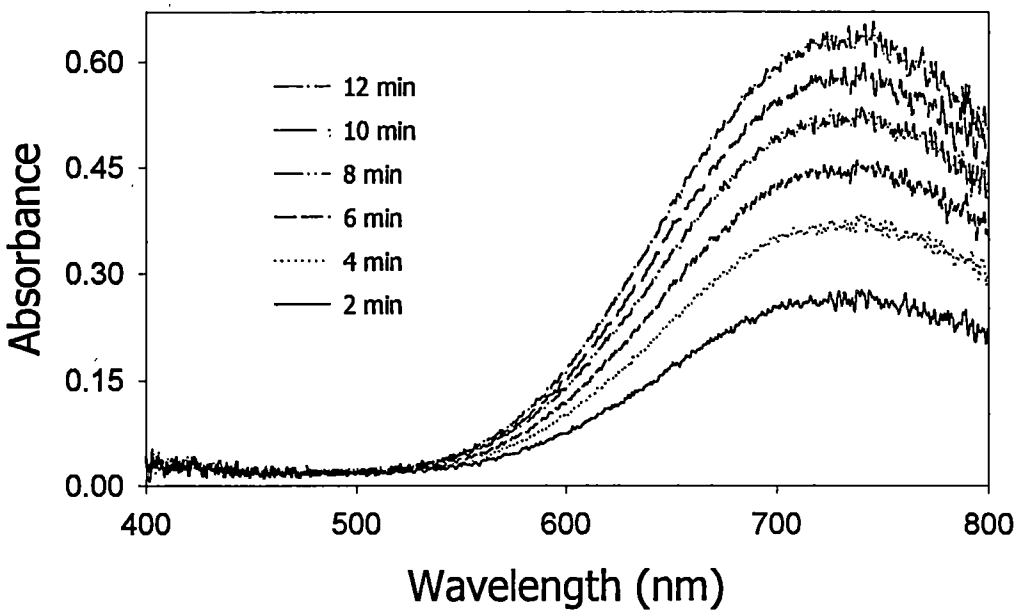

Figure 3.8. Absorbance spectra of a typical imprinted, monoamine ligand-grafted *gel 3-C* in 75.03 mM Cu^{2+} from 2-12 min.

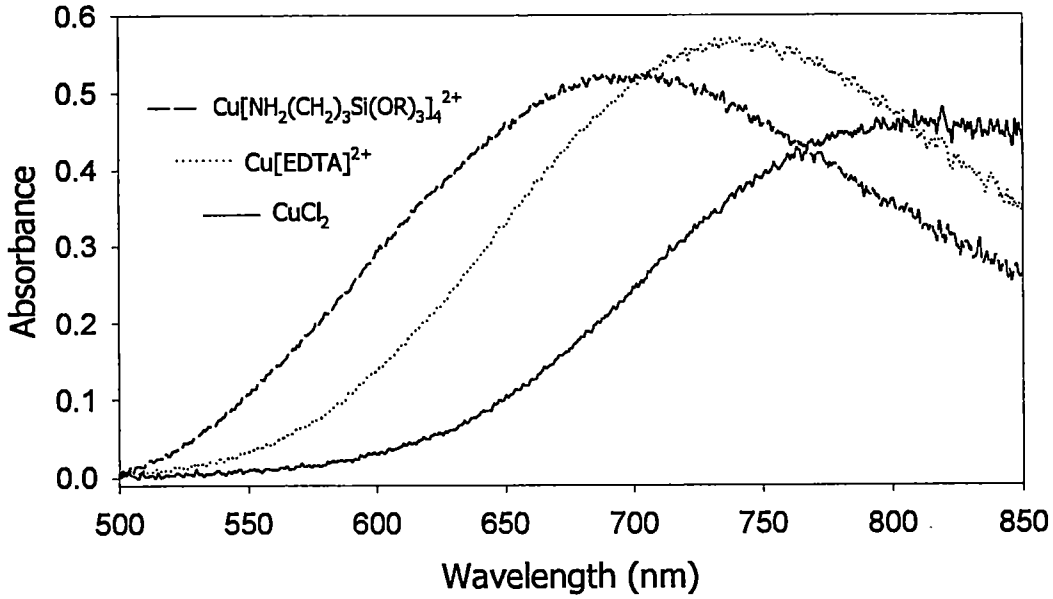

Figure 3.9. Absorbance spectra of $Cu[H_2N(CH_2)_3Si(OMe)_3]_4^{2+}$, $Cu[EDTA]^{2+}$, and $CuCl_2$ complexes.

Cu^{2+}:EDTA complex, a blank *gel 3-A* was placed in 0.100 M EDTA overnight and then rinsed with water before acquiring a spectrum. This gel showed no absorbance in the 730 nm region, indicating that the color change and absorbance observed was from the Cu^{2+}:amine complex within the gel and not due to a complex formed between Cu^{2+} and any residual EDTA. It is not clear what caused the shift in the wavelength of maximum absorbance of the Cu^{2+}:amine complex within the gel from 700 nm to 730 nm. It is possible that the immobilization of the complex into a solid sol-gel support may alter its spectroscopic properties. It is also possible that the broad $CuCl_2$ peak at 810 nm, which should be accounted for in the blank measurement, is not entirely subtracted from subsequent measurements and the broad peak seen at 730 nm is a combination of the $Cu[H_2N(CH_2)_3Si(OMe)_3]_4^{2+}$ complex at 700 nm and the $CuCl_2$ peak at 810 nm. However, it is important to note that λ_{max} for the complex within the gel did not change over the course of the experiment, i.e. no peak shift was observed.

Figure 3.10 shows typical plots of absorbance (*A*) at 730 nm vs. time (*t*) for several monoamine grafted, imprinted gels in various $[Cu^{2+}]$. The baseline absorbance of these plots has been offset for clarity. This approach relies on different Cu^{2+} diffusion rates in Cu^{2+} solutions of different concentrations. These plots are linear over a 10 min period ($R^2 > 0.98$) and show that as the $[Cu^{2+}]$ increases, the rate of Cu^{2+} diffusion into the gel, and thus the rate of formation of the blue Cu^{2+}:amine complex, also increases. The slopes of these lines can then be plotted against the concentration of

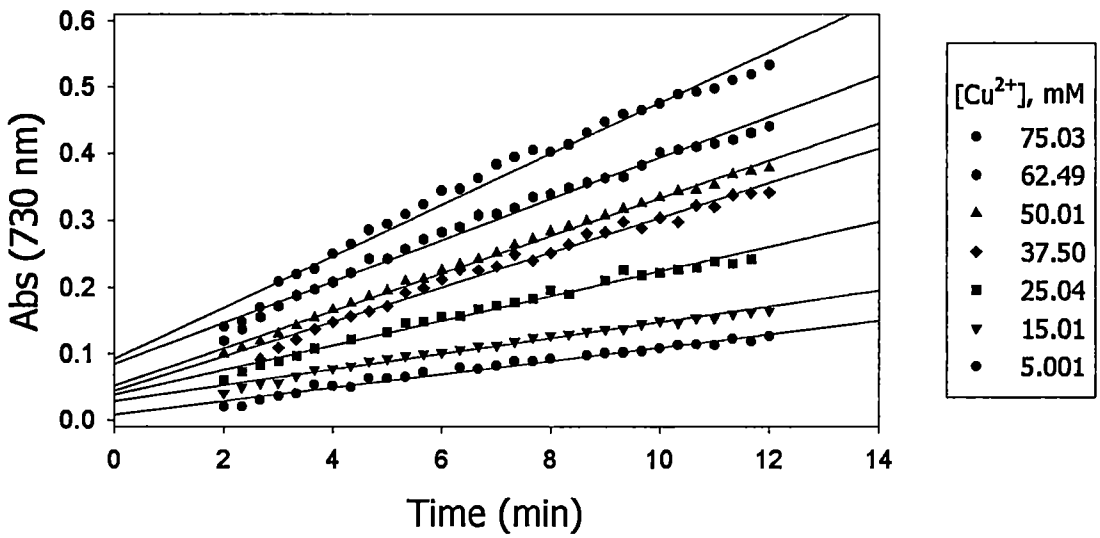

Figure 3.10. Absorbance vs. time plots of imprinted, monoamine ligand-grafted *gels 3-C* in various [Cu^{2+}] from 2-12 min. Baseline has been offset for clarity.

Cu^{2+} to obtain a calibration curve (**Figure 3.11**). Each point on the calibration curve is an average taken from at least five different gels. At 5.00-75.03 mM Cu^{2+}, the plot of *dA/dt* vs. [Cu^{2+}] is linear; however, above the concentration of 75.03 mM, the curve levels off. This is most likely due to a "bottle-neck" effect. The pores within the gel are only large enough to allow a given number of Cu^{2+} ions to diffuse into the gel interior per unit time. At high concentrations, there are more Cu^{2+} ions in solution, but only a limited number of these ions can diffuse into the gel and form a colored complex with the ligand. The limit of detection using this method was 5.00 mM Cu^{2+}; below this concentration, the absorbance signal of the gel could not be differentiated from background noise, and the slope of the absorbance vs. time plot did not change during the 10 min period studied.

The results for the monoamine grafted, imprinted gel sensors prepared in the same batch as well as between batches showed high reproducibility. Within a single Cu^{2+} uptake-removal cycle, the difference in *dA/dt* for gels of the same batch ranges from 0.32-5.2%. The data shown in the calibration curve is from three Cu^{2+} uptake-removal cycles of three separate batches of gels prepared at different times within 6 months. Each gel was stored in water for a different amount of time, and yet the results for these different gels were similar. In addition, the absorbance at several different wavelengths (700, 715, 725, 735, 745, and 760 nm) was studied, and the results obtained at these wavelengths were reproducible within experimental error, as shown in **Figure 3.12**.

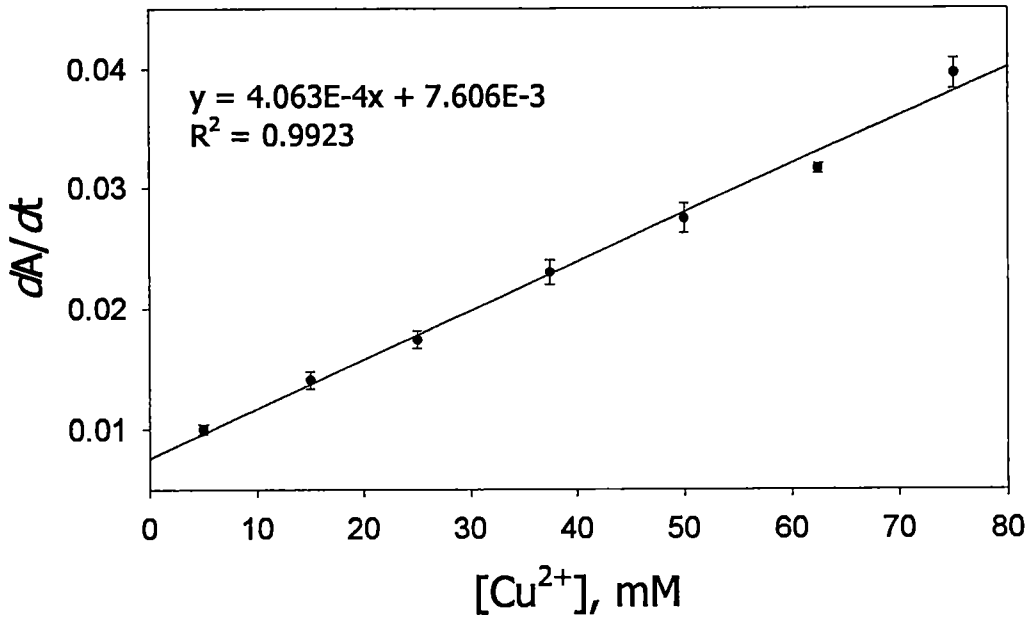

Figure 3.11. Correlation between slopes *dA/dt* from 2-12 min and $[Cu^{2+}]$ for imprinted, monoamine ligand-grafted *gels 3-C*.

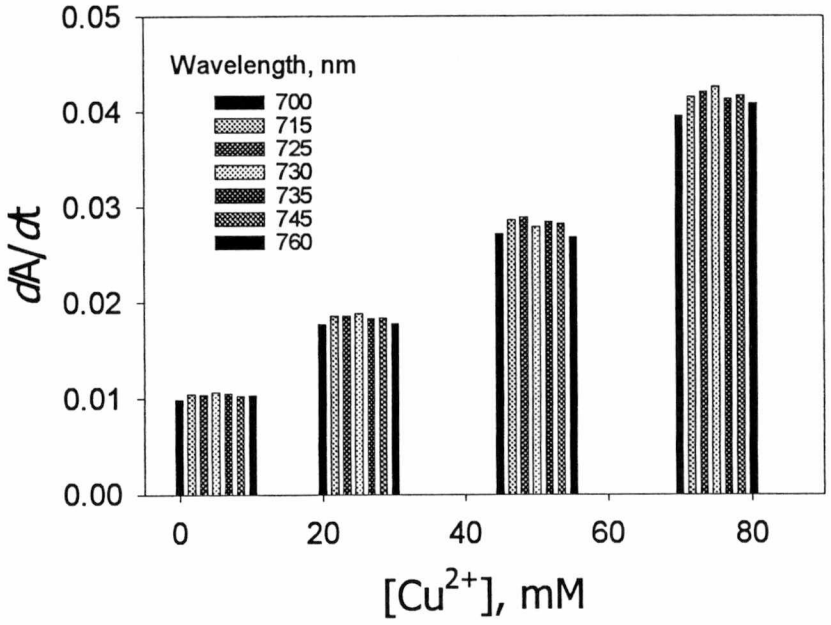

Figure 3.12. Difference in the correlation between dA/dt and $[Cu^{2+}]$ when the absorbance maximum is measured at several different wavelengths.

3.3.4 *Cu^{2+} Removal and Sensor Regeneration*

In order to develop a true optical ion sensor, the Cu^{2+} ions need to be removed from the gel between cycles. Reproducibility experiments from the diamine-grafted gels, discussed in Chapter 2, showed that Cu^{2+} ions could be removed from the gel using 1.0 M HCl. However, complete neutralization of these gels with base for use in subsequent Cu^{2+} uptake-removal cycles was not possible in the current studies, and results using these gels could not be reproduced over several cycles. Because of these difficulties, HCl was not used for gel regeneration in the monoamine ligand-grafted gels.

The stability constant, β, is defined by the following equation:

$$\beta = [ML_n]/ [M][L]^n \qquad \text{(Eq. 3.1)}$$

for the reaction shown by the chemical equation

$$M + nL \leftrightarrow ML_n \quad (M = \text{metal; } L = \text{ligand}) \qquad \text{(Eq. 3.2)}$$

and is often used to measure ligand affinity for the metal ion. A higher value of the stability constant indicates higher ligand affinity for the metal ion. For the complex $[Cu(NH_2CH_3)_4]^{2+}$, similar to the monoamine complex within the

gel, log β = 7.80, but for $[Cu(EDTA)]^{2+}$, log β = 18.8.[76] The stability constant for $[Cu(EDTA)]^{2+}$ is much higher than that for $[Cu(NH_2CH_3)_4]^{2+}$, indicating that Cu^{2+} will preferentially bind to EDTA, rather than to the monoamine ligand within the gel. This method of Cu^{2+} removal was not successful in the diamine-grafted gels discussed in Chapter 2 because log β = 20.3[76] for $[Cu(NH_2CH_2CH_2NH_2)]^{2+}$, indicating that the binding is stronger between Cu^{2+} and the diamine ligand within the gel than between Cu^{2+} and EDTA, and the EDTA solution would not likely remove Cu^{2+} ions from the gel. Because EDTA is inexpensive and readily available, and because it could easily be removed from the pores within the gel by simply washing with water, this solution was chosen for Cu^{2+} removal from the gel. **Table 3.1** shows the difference in *dA/dt* for four different gels taken through five cycles. When gels were regenerated with EDTA between spectral acquisitions, the capacity of the gels for Cu^{2+} uptake decreased slightly from one cycle to the next, but the difference in *dA/dt* plots was small over five cycles for a single gel, ranging from 4.0-7.9%.

3.4 Conclusions

The successful development of a reversible optical ion sensor for the determination of Cu^{2+} in flowing solutions has been described. The sol-gel process offers a simple, inexpensive route to physically stable monolithic optical sensors. The novel imprinting, ligand-grafting technique provided a

Table 3.1. Reproducibility of four gels (*gel 3-C*), each through five different cycles in 75.03 mM Cu^{2+} solution.

Cycle	*dA/dt* *
1	0.0422 ± 0.0007
2	0.0395 ± 0.0003
3	0.0377 ± 0.0008
4	0.0379 ± 0.0013
5	0.0367 ± 0.0018

* Four gels were used in each cycle to give the averages.

convenient way to modify the sol-gel sensor with a recognition element for the target metal ion. Our results showed that the sensors could be used to rapidly determine Cu^{2+} concentrations in the range of 5.00-75.03 mM with a low associated error. The sensor was regenerated easily using EDTA, and results were reproducible both from one gel to another and throughout several batches of gels over several cycles.

CHAPTER FOUR

CONCLUSIONS AND FUTURE STUDIES

4.1 Conclusions

Several different attempts in the preparation of sol-gel monoliths grafted with amine ligands for the determination of [Cu^{2+}] were demonstrated in Chapter 2. The challenges associated with the sol-gel processing of organic/inorganic hybrid materials were illustrated. Physically robust, optically transparent sol-gel discs containing functionalized amine ligands were prepared, and these discs could be used for the determination of Cu^{2+} in the concentration range of 5.00-91.02 mM with reasonable experimental error. However, these discs could not be regenerated and used in subsequent Cu^{2+} uptake/removal cycles and were therefore for single use only. Since these discs could be prepared in bulk simply and inexpensively from off-the-shelf chemicals and because results from sol-gel discs prepared by the same method at different times were reproducible, these disposable optical ion probes could be used in environmental field testing where fast, reliable results are necessary.

The successful development of a reversible optical ion sensor for the determination of Cu^{2+} in flowing solutions was described in Chapter 3. The sol-gel process offers a fast, convenient method for the preparation of

mechanically stable monolithic sensors for use in optical analysis. The novel imprinting, ligand-grafting technique provided a simple way to modify the sol-gel sensor with a recognition element for the target metal ion. Our results showed that the sensors could be used to determine Cu^{2+} concentrations in the range of 5.00-75.03 mM with a low associated error. The sensor was easily regenerated and results were reproducible from one gel to another over several cycles. This technique of analysis may be particularly useful in the electroplating or microelectronics industries where a reproducible sensor is desirable.

4.2 Future Studies

In the current studies, an *empirical* approach was employed that relates the rate of change in absorbance (*dA/dt*) of the copper(II)/ligand complexes to the Cu^{2+} concentration in solution. This approach has been used previously as a quantitative method of analysis.[41a,42] However, we found that the linear fit of the *dA/dt* plots was only valid during the initial time period when the gel was immersed in Cu^{2+} solution. After approximately 4 min, these curves deviate from linearity. We have conducted preliminary studies of a different approach, which is based on the kinetics of the diffusion of Cu^{2+} ions into the gel and their subsequent complexation with the immobilized ligands. The results of these preliminary studies are given in the appendix.

The techniques described in this thesis are only the first step in the development of an optical ion sensor for use in industry and in environmental field applications. Much of this initial work involved exploring the properties of functionalized sol-gel materials and the development of a sol-gel monolith of good optical quality for sensing applications. While we have shown that it is possible to prepare a sol-gel monolith grafted with recognition elements for ions of interest, and that these sensors show a correlation between the absorbance spectra of the complexes within their matrix and the concentration of metal ions in solution, more work should be conducted to optimize analytical parameters.

In the current studies, all experiments were conducted in pure aqueous $CuCl_2$ solutions of various concentrations. However, this chemical environment is not typical for most real-world applications. Industrial samples are likely to contain other chemical species, such as acids or bases, organic solvents, or other metal ions, within their matrix. The effect that these species have on the sensors described here has not been determined. It is possible that highly acidic conditions could cause the protonation of the amine groups within the gel, therefore diminishing Cu^{2+} binding. The amine ligands used in these studies are not selective only for Cu^{2+} ions, and the addition of other metals such as Ni^{2+} or Co^{2+} that could also form colored complexes with the ligands inside the gel would likely change the spectral characteristics of these sol-gel sensors. The influence of other chemicals within the sample matrix on the sensor performance

should be evaluated in order to develop a system that better represents industrial and environmental samples.

Indicating species other than the amine ligands illustrated in this work could also be encapsulated within the sol-gel matrix. Organic dyes may exhibit more intensely colored complexes with metal ions, offering the possibility of sol-gel thin films that might respond faster to metal ion concentrations. If the cocktail approach of incorporating different indicators selective for different metal ions into the sol-gel matrix together was employed, several different metal ion concentrations could be determined simultaneously with one sensor.

REFERENCES

(1) Greenwood, N. N.; Earnshaw, A. *Chemistry of the Elements*; 2nd ed.; Butterworth Heinemann: Oxford, 1998.

(2) Smith, B. W. *Sixty Centuries of Copper*; UK Copper Development Association: 1965.

(3) Copper Development Association, www.copper.org.

(4) *Environmental Health Criteria: Copper*; World Health Organization: Geneva, 1998; Vol. 200.

(5) Parthasaradhy, N. V. *Practical Electroplating Handbook*; Prentice Hall: Englewood Cliffs, 1989.

(6) Burgess, W. A. *Recognition of Health Hazards in Industry*; John Wiley and Sons: New York, 1995.

(7) Newman, L. S.; Newman, J. H. *Electroplating and Electroforming for Artists and Craftsmen*; Crown Publishers: New York, 1979.

(8) Gwennap, L. *Microprocessor Report* **1997**, *11*.

(9) Andricacos, P. C.; Uzoh, C.; Dukovic, J. O.; Horkans, J.; Deligianni, H. *IBM J. Res. Dev.* **1998**, *42*, 567-574.

(10) *IBM Introduces Advanced Chip Technology*, News, IBM Corporation, www.ibm.com/news/1997/09/ls9709222.html.

(11) Landau, U.; D'Urso, J.; Lipin, A.; Dordi, Y.; Malik, A.; Chen, M.; Hey, P. In *Electrochemical Processing in ULSI Fabrication and Semiconductor/Metal Deposition II*; Andricaos, P. C., Searson, P. C.,

Reidsema-Simpson, C., Allongue, P., Stickney, J. L., Oleszek, G. M., Eds.; The Electrochemical Society, 1999; Vol. 99-9, pp 25-39.

(12) *Trace Elements in Human Nutrition and Health*; World Health Organization: Geneva, 1996.

(13) Watson, J. S. *Separation Methods for Waste and Environmental Applications*; Marcel Dekker: New York, 1999.

(14) www.epa.gov

(15) Janata, J.; Josowicz, M.; Vanysek, P.; DeVaney, D. M. *Anal. Chem.* **1998**, *70*, 179R-208R.

(16) Janata, J. *Anal. Chem.* **2001**, *73*, 150A-153A.

(17) Wolfbeis, O. S. In *Fiber Optic Chemical Sensors and Biosensors*; Wolfbeis, O. S., Ed.; CRC Press: Boca Raton, 1991; Vol. 1, pp 1-23.

(18) Diamond, D. In *Chemical Analysis*; Winefordner, J. D., Ed.; John Wiley and Sons: New York, 1998; Vol. 150, pp 1-18.

(19) MacCraith, B. D. In *Chemical Analysis*; Winefordner, J. D., Ed.; John Wiley and Sons: New York, 1998; Vol. 150, pp 195-233.

(20) Avnir, D.; Braun, S.; Lev, O.; Levy, D.; Ottolenghi, M. In *Sol-Gel Optics Processing and Applications*; Klein, L., Ed.; Kluwer Academic: Norwell, Massachusetts, 1994; pp 539-582.

(21) Brinker, C. J.; Scherer, G. W. *Sol-Gel Science: The Physics and Chemistry of Sol-Gel Processing*; Academic Press: San Diego, 1990.

(22) Avnir, D.; Braun, S.; Ottolenghi, M. In *Supramolecular Architecture*, 1992; pp 384-404.

(23) Hench, L. L.; West, J. K. *Chem. Rev.* **1990**, *90*, 33-72.

(24) Buckley, A. M.; Greenblat, M. *J. Chem. Educ.* **1994**, *71*, 599-602.

(25) Avnir, D. *Acc. Chem. Res.* **1995**, *28*, 328-334.

(26) Lev, O. *Analusis* **1992**, *20*, 543-553.

(27) Harris, D. C. *Quantitative Chemical Analysis*; 4th ed.; W. H. Freeman and Company: New York, 1995.

(28) Skoog, D. A.; Holler, F. J.; Nieman, T. A. *Principles of Instrumental Analysis*; 5th ed.; Saunders College Publishing: Philadelphia, 1998.

(29) Ebsworth, E. A. V.; Rankin, D. W. H.; Cradock, S. *Structural Methods in Inorganic Chemistry*; 2nd ed.; CRC: Boca Raton, 1991.

(30) Huheey, J. E.; Keiter, E. A.; Keiter, R. L. *Inorganic Chemistry: Principles of Structure and Reactivity*; 4th ed.; Harper Collins: New York, 1993.

(31) Fagerlund, G. *Mater. Constr.* **1973**, *6*, 239-245.

(32) Quantachrome Corporation NOVA-1000 Gas Sorption Analyzer; 1992; pp 4.1-4.3, 4.5-4.6.

(33) Dollimore, D.; Spooner, P.; Turner, A. *Surf. Technol.* **1976**, *4*, 121-160.

(34) Sing, K. S. W.; Everett, D. H.; Haul, R. A. W.; Moscou, L.; Pierotti, R. A.; Rouquerol, J.; Siemieniewska, T. *Pure & Appl. Chem.* **1985**, *57*, 603-619.

(35) Flegler, S. L.; John W. Heckman, J.; Klomparens, K. L. *Scanning and Transmission Electron Microscopy: An Introduction*; W. H. Freeman and Company: New York, 1993.

(36) Watt, I. M. *The Principles and Practice of Electron Microscopy*; 2nd ed.; University Press: Cambridge, 1997.

(37) Breger, D. *Journeys in Microspace: The Art of the Scanning Electron Microscope*; Columbia University Press: New York, 1995.

(38) Nriagu, J. O. *Copper in the Environment*; John Wiley and Sons: New York, 1979; Vol. 1.

(39) Manahan, S. E. *Environmental Chemistry*; 6 Ed.; Lewis Publishers: Boca Raton, 1994.

(40) Boyle, E. A. In *Copper in the Environment*; Nriagu, J. O., Ed.; John Wiley and Sons: New York, 1979; Vol. 1, p 522.

(41) (a) Oehme, I.; Wolfbeis, O. *Mikrochim. Acta* **1997**, *126*, 177-192. (b) Seitz, W. R. In *Fiber Optic Chemical Sensors and Biosensors*; Wolfbeis, O. S., Ed.; CRC Press: Boca Raton, 1991; Vol. 2, pp 1-17.

(42) (a) Lu, J.; Zhang, Z. *Analyst* **1995**, *120*, 453-455. (b) Lu, J.; Zhang, Z. *Anal. Lett.* **1994**, *27*, 2431-2442.

(43) Saari, L. A.; Seitz, W. R. *Anal. Chem.* **1984**, *56*, 810-813.

(44) Preininger, C.; Wolfbeis, O. S. *Biosens. Bioelectron.* **1996**, *11*, 981-990.

(45) Wang, E.; Ohashi, K.; Kamata, S. *Chem. Lett.* **1992**, 939-942.

(46) Saito, T. *Talanta* **1994**, *41*, 811-815.

(47) Oehme, I.; Prokes, B.; Murkovic, I.; Werner, T.; Kilmant, I.; Wolfbeis, O. *Fresenius' J. Anal. Chem.* **1994**, *350*, 563-567.

(48) Im, H.-J.; Yang, Y.; Allain, L. R.; Barnes, C. E.; Dai, S.; Xue, Z. *Environ. Sci. Technol.* **2000**, *34*, 2209-2214.

(49) Tien, P.; Chau, L.-K. *Chem. Mater.* **1999**, *11*, 2141-2147.

(50) Mahmoud, M. E. *Anal. Lett.* **1996**, *29*, 1791-1804.

(51) Klonkowski, A. M.; Widernik, T.; Grobelna, B. *Mol. Eng.* **1995**, *5*, 381-389.

(52) Bien, T. In *ACS Symp. Ser.*; American Chemical Society: Washington, 1992; Vol. 499 (Supramolecular Architectures), pp 1-7.

(53) Dunn, B.; Zink, J. I. *J. Mater. Chem.* **1991**, *1*, 903-913.

(54) Allain, L. R.; Sorasaenee, K.; Xue, Z. *Anal. Chem.* **1997**, *69*, 3076-3080.

(55) Allain, L. R.; Xue, Z.; Roberts, M. J. *AT-PROCESS* **1998**, *3*, 98-103.

(56) Allain, L. R.; Xue, Z. *Anal. Chem.* **2000**, *72*, 1078-1083.

(57) Allain, L. R.; Xue, Z. *Anal. Chim. Acta* **2001**, *433*, 97-102.

(58) Brunauer, S.; Deming, L. S.; Deming, W. S.; Teller, E. *JACS* **1940**, *62*, 502-511.

(59) Burggraf, L. W.; Kendall, D. S.; Leyden, D. E.; Pern, F. J. *Anal. Chim. Acta* **1981**, *129*, 19-27.

(60) *MRS Bulletin* **1994**, *19* (Copper Metallization in Industry).

(61) Alkhatib, E.; O'Connor, T. *Am. Environ. Lab.* **1998**, *10*, 6-8.

(62) Ellis, A. B.; Walt, D. R. *Chem. Rev.* **2000**, *100* (Chemical Sensors).

(63) Lin, J.; Brown, C. W. *TrAC, Trends Anal. Chem.* **1997**, *16*, 200-211.

(64) Freeman, J. E.; Childers, A. G.; Steele, A. W.; Hieftje, G. M. *Anal. Chim. Acta* **1985**, *177*, 121-128.

(65) Lu, J.; Zhang, Z. *Electrochem. J.* **1995**, *52*, 315-319.

(66) Bright, F. V.; Poirier, G. E.; Hieftje, G. M. *Talanta* **1988**, *35*, 113-118.

(67) Qin, W.; Zhang, Z.; Liu, H. *Anal. Chem.* **1998**, *70*, 3579-3584.

(68) Wulff, G. *Agnew. Chem. Int. Ed. Engl.* **1995**, *34*, 1812-1832.

(69) Shea, K. J. *Trends Polym. Sci.* **1994**, *2*, 166-173.

(70) Bartsch, R. A.; Maeda, M. *ACS Symposium Series*; American Chemical Society: Washington, 1998; Vol. 703 (Molecular and Ionic Reognition with Imprinted Polymers).

(71) Dai, S.; Burleigh, M. C.; Shin, Y.; Morrow, C. C.; Barnes, C. E.; Xue, Z. *Agnew. Chem. Int. Ed.* **1999**, *38*, 1235-1239.

(72) Dai, S.; Shin, Y.; Ju, Y.; Burleigh, M. C.; Lin, J.-S.; Barnes, C. E.; Xue, Z. *Adv. Mater.* **1999**, *11*, 1226-1230.

(73) Dai, S.; Burleigh, M. C.; Ju, Y. H.; Gao, H. J.; Lin, J. S.; Pennycook, S. J.; Barnes, C. E.; Xue, Z. L. *JACS* **2000**, *122*, 992-993.

(74) Burleigh, M. C. *Molecular Imprinting of Organofunctionalized Sol-Gel Materials for Metal Ion Separations*; Ph. D. Dissertation, University of Tennessee, Knoxville: 2000; p 249.

(75) Klonkowski, A. M.; Grobelna, B.; Widernik, T.; Jankowska-Frydel, A.; Mozgawa, W. *Langmuir* **1999**, *15*, 5814-5819.

(76) Bjerrum, J.; Schwarzenbach, G.; Sillen, L. G. *Stability Constants of Metal-Ion Complexes, with Solubility Products of Inorganic Substances*; Metcalfe and Cooper Limited: London, 1957; Vol. 1 (Organic Ligands).

APPENDIX

DIFFUSION-BASED COPPER (II) SENSOR RESPONSE

In the studies described in this thesis, an empirical approach was adopted that related the rate of change in absorbance of the complexes within the sol-gel (*dA/dt*) to the Cu^{2+} concentration in solution. Such an approach has been used in other sensor systems.[A-1] However, the linear fit of the *dA/dt* plots was found valid only during the initial time period when the gel was immersed in Cu^{2+} solution; after approximately 4 min, the *dA/dt* plots deviated from linearity. The plots could be described with a polynomial curve fit, but a less empirical method of describing these plots was desired. The results of preliminary studies using a theoretical approach based on the kinetics of the diffusion of Cu^{2+} ions into the gel and their later complexation with the immobilized amine ligands are presented herein.

A.1 Assumptions

(a) A diagram of the sol-gel sensor disk is shown in **Figure A.1**. Cu^{2+} diffusion is mainly along the *x* direction from both sides of the gel. The diffusion from the top and bottom of the gel is ignored, as $2r > 2l$ and the area detected by the fiber optic device is small and centered.

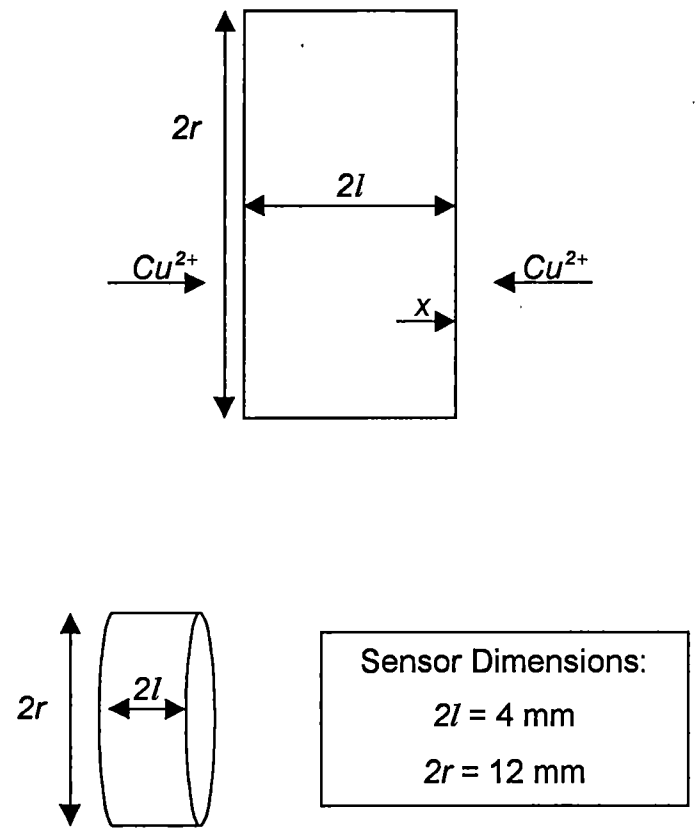

Figure A.1. Dimensions of a sol-gel sensor disk.

(b) The imprinted ligand environment in the gel, illustrated in below, is treated as one "macrocyclic ligand," denoted as L. The initial concentration of this ligand is $C_{L,0}$.

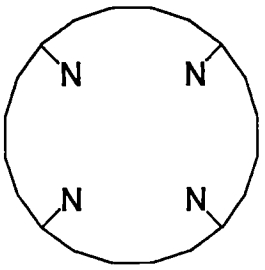

$\equiv$ L

A.2 Concentrations of the Ligand, L, and the Complex

The concentrations of the ligand L and the complex within the gel are described by the following equations:

$$C_{complex} + C_L = C_{L,0} \qquad C_L: \text{concentration of } L \qquad \text{(Eq. A.1)}$$

$$Cu^{2+} + L \underset{k_b}{\overset{k_f}{\rightleftharpoons}} CuL^{2+} \qquad K = \frac{k_f}{k_b} \qquad \text{(Eq. A.2)}$$

$$K = \frac{[CuL^{2+}]}{[Cu^{2+}][L]} = \frac{C_{complex}}{C_{Cu^{2+}}C_L} =$$

$$\frac{C_{complex}}{C_{Cu^{2+}}(C_{L,0}-C_{complex})} = \frac{(C_{L,0}-C_L)}{C_{Cu^{2+}}C_L} \qquad \text{(Eq. A.3)}$$

Thus,

$$C_{complex} = \frac{KC_{Cu^{2+}}C_{L,0}}{1 + KC_{Cu^{2+}}} \qquad \text{(Eq. A.4a)}$$

and

$$C_L = \frac{C_{L,0}}{1 + KC_{Cu^{2+}}} \qquad \text{(Eq. A.4b)}$$

A.3 Kinetic Model

Fick's laws of diffusion are a set of differential equations describing the flux of a substance and its concentration (C) as functions of time (t) and position (x).[A-2] Fick's Second Law of Diffusion states that:

$$\frac{\partial C(x,t)}{\partial t} = D\frac{\partial^2 C(x,t)}{\partial x^2} \qquad \text{(Eq. A.5)}$$

where $C(x,t) = C_{Cu}^{2+}$ and D represents the diffusion coefficient. This is derived from Fick's First Law of Diffusion, which states that the flux is proportional to the concentration gradient in the following:

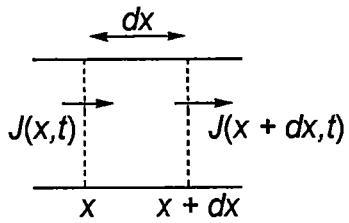

where J = the flux of Cu^{2+}. Fick's First Law of Diffusion may then be stated as:

$$-J(x,t) = D\frac{\partial C(x,t)}{\partial x} \qquad \text{(Eq. A.6)}$$

In the current system, Cu^{2+} ions in the element of dx react with L to form the complex CuL^{2+}. The rate of this reaction is $k_f C(x,t) C_L$. Thus,

$$\frac{\partial C(x,t)}{\partial t} = D\frac{\partial^2 C(x,t)}{\partial x^2} - k_f C(x,t) C_L \qquad \text{(Eq. A.7a)}$$

Using Eq. A.4b:

$$\frac{\partial C(x,t)}{\partial t} = D\frac{\partial^2 C(x,t)}{\partial x^2} - k_f C(x,t)\frac{C_{L,0}}{[1+KC(x,t)]} \qquad \text{(Eq. A.7b)}$$

Assuming that, except at the early stage of diffusion, when $C(x,t)$ is exceedingly small ($<10^{-13}$ or 10^{-20} M, respectively, for monoamine and diamine grafted gels),

$$1+KC(x,t) \approx KC(x,t) \qquad \text{(Eq. A.8)}$$

as K is approximately 10^{13} for $Cu(NH_3)_4^{2+}$ and 10^{20} for $Cu(en)_2^{2+}$.[A-3] The reason for making the approximation in Eq. A.8 is that the $k_f C(x,t) C_{L,0} / [1 + kC(x,t)]$ term needs to be linear with respect to $C(x,t)$ in order to have a closed form solution, other than appropriate numerical solutions,[A-4] for the partial differential equation in Eq. A.7b.[A-4] Eq. A.7b therefore changes to:

$$\frac{\partial C(x,t)}{\partial t} = D\frac{\partial^2 C(x,t)}{\partial x^2} - k \qquad \text{(Eq. A.9)}$$

where $k = k_b C_{L,0}$.

The partial differential equation in Eq. A.9 could be solved with the use of Laplace transformation[A-5] or Fourier series,[A-6] after the boundary and initial conditions in Eqs. A.10-A.12 are applied.

$C(0,t) = C_0$ (Cu^{2+} concentration in the bulk) (Eq. A.10)

$C(2l,t) = C_0$ (Cu^{2+} concentration in the bulk) (Eq. A.11)

$C(x,0) = 0$ (Eq. A.12)

The solution thus gives the Cu^{2+} concentration as a function of position x and time t.

$C_{Cu}^{2+} = C(x,t)$ (Eq. A.13)

A.4 Absorbance of the Sensor Monolith

When dx is defined as follows,

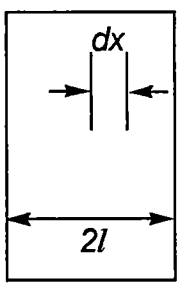

the contribution of the infinitely small unit dx to absorbance, A, is dA. From Beer's Law, assuming the two sides of the gel are equal:

$dA = 2\varepsilon C_{complex} dx$ (Eq. A.14)

From Eq. A.4a,

$$C_{complex} = C_{L,0}\left(1 - \frac{1}{1 + KC_{Cu^{2+}}}\right) = C_{L,0}\left\{1 - \frac{1}{1 + KC(x,t)}\right\} \qquad \text{(Eq. A.15)}$$

$$A = 2\varepsilon C_{L,0}\int_0^l \left\{1 - \frac{1}{1 + KC(x,t)}\right\} dx \qquad \text{(Eq. A.16)}$$

Eq. A.16 gives absorbance A as a function of time t and Cu^{2+} concentration in the bulk (C_0):

$$A = A(t,\ C_0) \qquad \text{(Eq. A.17)}$$

Thus, using a standard solution with known C_0 and measuring the absorbance, A, at time t, Eq. A.17 gives:

$$\begin{aligned} A_1 &= A(t_1, C_0) \\ A_2 &= A(t_2, C_0) \\ &\cdot \\ &\cdot \\ A_n &= A(t_n, C_0) \end{aligned} \qquad \text{(Eq. A.18)}$$

These equations will yield the constants ε, $C_{L,0}$, D, k, and K.

For an unknown solution (a solution with unknown C_0), experiments will give a set of *(A, t)* equations, such that

$$A_1 = A(t_1, C_0)$$
$$A_2 = A(t_2, C_0)$$
$$\vdots$$
$$A_n = A(t_n, C_0) \qquad \text{(Eq. A.18)}$$

These equations will give C_0.

REFERENCES FOR THE APPENDIX

(A-1) (a) Oehme, I.; Wolfbeis, O. *Mikrochim. Acta* **1997**, *126*, 177-192. (b) Seitz, W. R. In *Fiber Optic Chemical Sensors and Biosensors*; Wolfbeis, O. S., Ed.; CRC Press: Boca Raton, 1991; Vol. 2, pp 1-17. (c) Lu, J.; Zhang, Z. *Analyst* **1995**, *120*, 453-455. (d) Lu, J.; Zhang, Z. *Anal. Lett.* **1994**, *27*, 2431-2442.

(A-2) Bayrd, A. J.; Faulkner, L. R. *Electrochemical Methods: Fundamentals and Applications*; John Wiley and Sons: New York, 1980.

(A-3) Bjerrum, J.; Schwarzenbach, G.; Sillen, L. G. *Stability Constants of Metal-Ion Complexes, with Solubility Products of Inorganic Substances*; Metcalfe and Cooper Limited: London, 1957; Vol. 1 (Organic Ligands).

(A-4) Eriksson, K.; Estep, D.; Hansbo, P.; Johnson, C. *Computational Differential Equations*; Cambridge University Press: New York, 1996.

(A-5) Churchill, R. V. *Operational Mathematics*; McGraw-Hill: New York, 1958.

(A-6) Churchill, R. V.; Brown, J. W. *Fourier Series and Boundary Value Problems*; 3rd Ed, McGraw-Hill: New York, 1978.

VITA

Cheri Whitehead Clavier was born in Elizabethton, Tennessee on August 13, 1975. She attended schools in the public school systems of Elizabethton and Carter County, Tennessee, where she graduated with honors from Elizabethton High School in May of 1993. She graduated *cum laude* with a Bachelor of Science degree in Chemistry from East Tennessee State University in May of 1998. She entered graduate school at The University of Tennessee in August of 1998; it was here that she met her future husband. Under the direction of Dr. Ziling (Ben) Xue, she successfully developed mechanically stable sol-gel monoliths for the optical determination of copper (II) ions in flowing solutions. She earned a Master of Science degree in Chemistry with an emphasis in Analytical Chemistry in December of 2001. A lifetime student, she is currently pursuing a Master of Science degree in Science Education with a concentration in Secondary Teaching at The University of Tennessee, Knoxville.